Simulation of spirits distillation for a better understanding of volatile aroma compounds behavior: Application to Armagnac production

Cristian Puentes[a], *Xavier Joulia*[b], *Jean-Paul Vidal*[c], *Martine Esteban-Decloux*[a,*]

[a] *Unité Mixte de Recherche Ingénierie Procédés Aliments, AgroParisTech, INRA, Université Paris-Saclay, F-91300 Massy, France*

[b] *Laboratoire de Génie Chimique, Université de Toulouse INPT-ENSIACET, CNRS, F-31030 Toulouse, France*

[c] *Union Nationale de Groupements de Distillateurs d'Alcool, F-92240 Malakoff, France*

A B S T R A C T

A methodology for the simulation of spirits continuous distillation was developed and applied to the analysis of an Armagnac unit, using the software ProSimPlus®. Distillation data for 66 aroma compounds were acquired during an experimental campaign and 32 of these species were simulated with the NRTL model, using interaction parameters estimated from equilibria data at high dilution.

Validation of static simulations against reconciled experimental data showed that the recovery of aroma compounds from wine to distillate can be predicted with good precision. Considering relative volatilities and composition profiles, three main groups of aroma compounds were proposed: (I) light compounds (recovered in distillate), (II) intermediary compounds (distributed between distillate and vinasse) and (III) heavy compounds (recovered in vinasse).

After validation of the nominal point, the influence of some operating parameters was investigated. According to simulation, three parameters, namely, tails extractions, ethanol concentration in distillate and distillate temperature, have a real impact on Spirit composition. They permit a preferential reduction of intermediary and heavy species with respect to ethanol. Comparison with experimental and literature data confirms that simulation is a powerful and reliable approach to analyze the synergy between process operation, its performance and Spirit composition.

1. Introduction and state of the art

Spirits are alcoholic beverages produced from different agricultural raw materials, such as apple and pear (Calvados), barley (Whisky), grape (Cognac, Armagnac, Pisco) and sugar cane juice (Rum, Cachaça). For most commercial spirits, the production process is comprised of five main stages: raw material extraction, yeast fermentation, distillation of the fermented wash, ageing of the distillate in wooden barrels and final dilution to adjust the ethanol content to the desired level (Nykänien and Suomalainen, 1983; Carrau et al., 2008; Franitza et al., 2016).

In France, four main spirits are produced: Armagnac, Calvados, Cognac and Martinique agricultural rum. They are protected by the French label AOC (*Appellation d'Origine Contrôlée*), which delimits the production areas as well as the rules

for their fabrication. Besides the raw material, the major differences among these distilled beverages are the geographic regions of production and distillation methods (Decloux and Joulia, 2009; Ledauphin et al., 2010).

From a chemical point of view, spirits are complex mixtures composed by an ethanol–water liquid matrix and a great variety of volatile compounds present at low concentrations. Many commercial spirits also contain substantial amounts of non-volatile material from ageing and finition (MacNamara and Hoffmann, 1998; MacNamara et al., 2010). The volatile compounds, also known as congeners, are organic species from chemical families including acetals, alcohols, carbonyl compounds, carboxylic acids, esters, furans, norisoprenoids, sulphur compounds and terpenes. Some of them are derived from the original raw material or the extraction phase, but the majority are generated during fermentation and distillation, phases in which complex reactions take place. The alcoholic fermentation, main reaction of the process, leads together with ethanol, to the synthesis of the most abundant congeners (alcohols, fatty acids and their esters). Other involved reactions are malolactic fermentation, acetalization, ester hydrolysis, esterification, Maillard reaction, Stecker degradation and thermal degradation of pentoses (Cantagrel et al., 1990; Sourisseau, 2002). Finally, the ageing phase also contributes to the complexity of spirits, with the formation of new volatile compounds from wood constituents, including phenolic compounds and lactones (Guymon, 1974; Maarse and Van Den Berg, 1994; Rodriguez et al., 2003; Ferrari et al., 2004).

The volatile species are also referred to as volatile aroma compounds because their presence and composition play an essential role on spirits quality (Guymon, 1974; Nykänen, 1986; Guichard et al., 2003; Ferrari et al., 2004; Apostolopoulou et al., 2005; Ledauphin et al., 2006, 2010; Morakul et al., 2011; Franitza et al., 2016). This quality is associated to the organoleptic properties of the product, such as flavor and aroma. Its evaluation and control are therefore essential for production purposes, as it influences the consumer preferences (Maarse and Van Den Berg, 1994). The relationship between aroma and spirits composition is very complex because of the variety of volatile compounds, their variable naturally occurring concentrations and their combined effects. Indeed, the sensory influence of each species depends on a triple factor: its concentration, its sensory threshold value and the concentration of other species in the solution. As a result, the contribution of trace level compounds with low sensory threshold to aroma and flavor may be more important than the impact of the most abundant volatile compounds. Nevertheless, analysis of these latter species is important, not only to describe the main character of the product, but also to evaluate the production continuity and product authenticity (MacNamara and Hoffmann, 1998; MacNamara et al., 2010).

In light of these facts, the control of volatile aroma compounds content in distillates is a factor that contributes to the production of good quality spirits. The composition control is also important in matters of food safety, as the presence of specific volatile aroma compounds at high concentrations, for instance methanol and ethanal, is related to some health issues (Nykänen, 1986; Paine and Dayan, 2001). Considering its origin, the control of volatile aroma compounds composition can be performed by manipulating two factors: the raw material or the production process. Some recent experimental works have demonstrated the high dependency between this latter factor and product composition (Rodriguez et al., 2003; Cacho et al., 2013; Franitza et al., 2016), which opens up prospects for the improvement of spirits production.

Focusing on the distillation stage, spirits can be produced by continuous multistage distillation or batch distillation (Decloux and Joulia, 2009; Piggott, 2009). Currently, the adaptation and evolution of this process remains very limited, as the operation of the distillation units is mainly based on traditional methods derived from empirical knowledge. Thus, the implementation of chemical engineering methods, in particular process simulation, turns out be an efficient approach to represent, understand and optimize this separation process for a better quality control (Batista and Meirelles, 2011; Valderrama et al., 2012b; Esteban-Decloux et al., 2014).

Although the implementation of process simulators in food processing is relatively scarce, due to the complexity of the involved phenomena and the lack of property data (Joulia, 2008; Bon et al., 2009), several works dealing with simulation of alcoholic continuous and batch distillations have been reported in the open literature. A synthesis of the main reports published since 2000 is presented in Table 1. This synthesis includes studies on diverse spirits: Cachaça (Scanavini et al., 2010, 2012; Batista and Meirelles, 2011), Fruits spirits (Claus and Berglund, 2009), Pisco (Osorio et al., 2004; Carvallo et al., 2011), Whisky (Gaiser et al., 2002; Valderrama et al., 2012b), pear distillate (Sacher et al., 2013) and bitter orange distillate (Esteban-Decloux et al., 2014). Works on bioethanol (Batista and Meirelles, 2009; Batista et al., 2012, 2013; Tgarguifa et al., 2017), neutral alcohol (Decloux and Coustel, 2005; Valderrama et al., 2012b; Batista et al., 2013; Esteban-Decloux et al., 2014) and anhydrous ethanol (Bastidas et al., 2012) are also summarized, as these products are also derived from agricultural raw material, sugar cane juice and molasses in this specific case.

Two kinds of simulation tools were used in these works: commercial simulators (including AspenPlus®, Aspen Dynamics®, BatchColumn®, ChemCAD® and ProSimPlus®) or in-house made simulators developed by the authors. In both cases, the simulator is a software that permits the representation of the distillation process through a model that involves the mass and energy balances, coupled to phase equilibria and, in some cases, transport equations and chemical reactions (Gil et al., 2011).

In most of these researches two common points can be outlined:

- The objective of the simulation is to represent accurately the distillation units and to gain better insight into the ethanol and congeners distillation as well as process performance.
- The fermented wash and subsequent process streams are represented as a simplified ethanol–water mixture containing some of the major volatile aroma compounds common to most spirits, namely: 1,1-diethoxyethane, methanol, prop-2-en-1-ol, propan-1-ol, propan-2-ol, 2-methylpropan-1-ol, butan-1-ol, butan-2-ol, 2-methylbutan-1-ol, 3-methylbutan-1-ol, pentan-1-ol, pentan-2-ol, hexan-1-ol, 2-phenylethanol, ethanal, propan-2-one, ethanoic acid, propanoic acid, octanoic acid, methyl ethanoate, ethyl ethanoate, ethyl hexanoate, ethyl decanoate and furan-2-carbaldehyde, α-pinene, limonene, linalool and linalool oxide. The number of volatile aroma compounds included in the simulations varies from zero (only binary ethanol–water, Claus and Berglund, 2009) to 16 (Batista et al., 2012; Batista et al., 2013). Some works also considered non-volatile species, such as glycerol (Bastidas et al., 2012; Tgarguifa et al., 2017), and carbon dioxide, which constitutes the major

Table 1 – Research works published in the open literature since 2000 on simulation of alcohol distillation.

	Authors	Aim of the study	Simulation tool	Thermodynamic approach	Solution model
Continuous distillation	Gaiser et al., 2002 *Whisky*	- Representation of a patent unit (two columns). Comparison with literature data.	AspenPlus	*Vapor phase:* Ideal gas *Liquid phase:* NRTL	*Solvent:* ethanol, water *Aroma compounds:* propan-1-ol, 2-methylpropan-1-ol, 3-methylbutan-1-ol; ethanal
	Decloux and Coustel, 2005 *Neutral alcohol*	- Representation of an industrial plant (seven columns) and understanding of the role of the distillation units, regarding ethanol and aroma compounds behaviour. No comparison with experimental data.	ProSimPlus	*Vapor phase:* Ideal gas *Liquid phase:* UNIFAC	*Solvent:* ethanol, water *Aroma compounds:* methanol, propan-1-ol, 2-methylpropan-1-ol, 3-methylbutan-1-ol; ethanal; ethyl ethanoate
	Batista and Meirelles, 2009 *Bioethanol*	- Representation of an industrial plant (three columns) and analysis of the influence of operating conditions upon the concentration profiles in the distillation units. No comparison with experimental data. - Design of strategies for controlling the ethanal content in bioethanol using a PID controller, a degassing system as well as a new system configuration with two supplementary columns producing a second alcohol stream.	Aspen Plus and Aspen Dynamics	*Vapor phase:* Virial equation coupled to the Hayden-O'Connell model *Liquid phase:* NRTL	*Solvent:* ethanol, water *Aroma compounds:* methanol, propan-1-ol, propan-2-ol, 2-methylpropan-1-ol, 3-methylbutan-1-ol; ethanal; ethanoic acid; ethyl ethanoate *Other compounds:* Carbon dioxide
	Batista and Meirelles, 2011 *Cachaça*	- Representation of two industrial plants (1. Classic installation with one column, and a degassing system; 2. Pasteurized installation with one main column, one side column, and a degassing system) and analysis of the influence of operating parameters upon the product quality. Comparison with own experimental data. - Design of strategies for controlling the volatile content in the spirit using a PID controller linked to the degassing system.	Aspen Plus and Aspen Dynamics	*Vapor phase:* Virial equation coupled to the Hayden-O'Connell model *Liquid phase:* NRTL	*Solvent:* ethanol, water *Aroma compounds:* methanol, propan-1-ol, propan-2-ol, 2-methylpropan-1-ol, 3-methylbutan-1-ol; ethanal, propan-2-one; ethanoic acid; ethyl ethanoate *Other compounds:* Carbon dioxide
	Batista et al., 2012 *Bioethanol*	- Representation of an industrial plant (two columns with degassing systems, and a decanter), understanding of aroma compounds behavior and analysis of the influence of operating and constructive variables on its performance, for the optimization of the equipment's configuration. Comparison with own experimental data. - Development of control loops to compensate changes in wine concentration and prevent off-specification products	Aspen Plus and Aspen Dynamics	*Vapor phase:* Virial equation coupled to the Hayden-O'Connell model *Liquid phase:* NRTL	*Solvent:* ethanol, water *Aroma compounds:* methanol, propan-1-ol, propan-2-ol, 2-methylpropan-1-ol, butan-1-ol, butan-2-ol, 2-methylbutan-1-ol, 3-methylbutan-1-ol, pentan-1-ol, hexan-1-ol; ethanal, propan-2-one; ethanoic acid, propanoic acid; methyl ethanoate, ethyl ethanoate *Other compounds:* carbon dioxide
	Bastidas et al., 2012 *Anhydrous fuel ethanol*	- Representation of an industrial plant (four distillation columns) and analysis of the influence of operating parameters upon its performance. Comparison with own experimental data. - Performance of thermal and hydraulic studies of the distillation columns to evaluate the possibility of expanding the net production rate.	AspenPlus	*Vapor phase:* Predictive Soave-Redlich-Kwong equation of state *Liquid phase:* NRTL	*Solvent:* ethanol, water *Aroma compounds:* methanol, propan-1-ol, propan-2-ol, 2-methylpropan-1-ol, butan-1-ol, 3-methylbutan-1-ol, pentan-1-ol; ethanal; ethanoic acid *Other compounds:* carbon dioxide

– Table 1 (*Continued*)

	Authors	Aim of the study	Simulation tool	Thermodynamic approach	Solution model
Discontinuous distillation	Valderrama et al., 2012b *Neutral alcohol*	- Representation of an industrial plant (two columns and a light component separator) and analysis of the influence of feed beer composition on the composition profiles and product quality. Comparison with literature data.	ChemCAD	*Vapor phase:* Ideal gas *Liquid phase:* NRTL	*Solvent:* ethanol, water *Aroma compounds:* methanol, propan-1-ol, butan-1-ol, 3-methylbutan-1-ol, pentan-2-ol, acetic acid *Other compounds:* carbon dioxide, propane-1,2,3-triol
	Batista et al., 2013 *Bioethanol, Neutral alcohol*	- Representation of an industrial plant and analysis of the influence of operating and constructive conditions upon the purification of fuel bioethanol. Comparison with own experimental data. - Development of a new plant for neutral alcohol production considering the required quality standards and operating performance. Comparison with literature data.	Aspen Plus	*Vapor phase:* Virial equation coupled to the Hayden-O'Connell model *Liquid phase:* NRTL	*Solvent:* ethanol, water *Aroma compounds:* methanol, propan-1-ol, propan-2-ol, 2-methylpropan-1-ol, butan-1-ol, butan-2-ol, 2-methylbutan-1-ol, 3-methylbutan-1-ol, pentan-1-ol, hexan-1-ol; ethanal, propan-2-one; ethanoic acid, propanoic acid; methyl ethanoate, ethyl ethanoate *Other compounds:* carbon dioxide
	Esteban-Decloux et al., 2014 *Neutral alcohol*	- Representation of an industrial plant (four distillation columns, and a decanter) and understanding of the aroma compounds behavior. Comparison with own experimental data. - Determination of new operation points to maximize productivity and improve product quality.	ProSimPlus	*Vapor phase:* Ideal gas *Liquid phase:* NRTL	*Solvent:* ethanol, water *Aroma compounds:* 1,1-diethoxyethane; methanol, prop-2-en-1-ol, propan-1-ol, 2-methylpropan-1-ol, butan-1-ol, butan-2-ol, 3-methylbutan-1-ol; ethanal; ethyl ethanoate
	Tgarguifa et al., 2017 *Bioethanol*	- Representation of an industrial plant (three vacuum columns) and analysis of operating conditions for the optimization of the energy consumption and operating costs. Comparison with own experimental data.	In-house made model (including equations of: mass balance, heat balance, thermodynamic equilibrium and summation)	*Vapor phase:* Virial equation coupled to the Hayden-O'Connell model *Liquid phase:* NRTL	*Solvent:* ethanol, water *Aroma compounds:* ethanal; ethanoic acid *Other compounds:* propane-1,2,3-triol
	Osorio et al., 2004 *Pisco*	- Evaluation of a simulation strategy using artificial neural networks, with respect to the computing efficiency and accuracy in the representation of composition profiles. No comparison with experimental data.	In-house made differential model (including equations of: mass balance, heat balance, thermodynamic equilibrium, liquid hydraulics, liquid density, and reaction kinetics for some components)	*Vapor phase:* Ideal gas *Liquid phase:* Van Laar (Solvent), UNIFAC (aroma compounds)	*Solvent:* ethanol, water *Aroma compounds:* methanol; octanoic acid; ethyl hexanoate; linalool
	Claus and Berglund, 2009 *Fruits spirits*	- Setting of the operating parameters (reflux ratio, average distillate flow rate and time cutoff frames) required in the different operation steps for the simulation of two distillation units (one lab-scale and one pilot-scale). Adjustment and comparison with own experimental data.	ChemCAD	*Vapor phase:* Ideal gas *Liquid phase:* Comparison of NRTL and UNIFAC	*Solvent:* ethanol, water

Scanavini et al., 2010 *Cachaça*	- Estimation of the temperature and ethanol composition profiles in the distillate as well as aroma compounds concentrations in different cuts of a lab-scale distillation unit (charentais alembic). Comparison with own experimental data.	In-house made differential model (including equations of: mass balance, heat balance, thermodynamic equilibrium and heat losses)	*Vapor phase:* Virial equation coupled to the Hayden-O'Connell model *Liquid phase:* NRTL	*Solvent:* ethanol, water *Aroma compounds:* methanol, propan-1-ol, 2-methylpropan-1-ol, 3-methylbutan-1-ol; ethanal; ethanoic acid; ethyl ethanoate
Carvallo et al., 2011 *Pisco*	- Evaluation of a simulation strategy, with respect to ethanol composition profile, methanol concentration in different cuts and some operating variables in a pilot-scale distillation unit (composed of a boiler, a packed column and a partial condenser). Comparison with literature data as well as own experimental data.	In-house made differential model (including equations of: mass balance, heat balance, thermodynamic equilibrium, mass transfer and liquid properties)	*Vapor phase:* Ideal gas *Liquid phase:* NRTL	*Solvent:* ethanol, water *Aroma compounds:* methanol
Scanavini et al., 2012 *Cachaça*	- Determination and understanding of ethanol and aroma compounds compositions profiles in the distillate as well as some operation parameters of a lab-scale distillation unit (charentais alembic). Comparison with own experimental data. - Experimental determination of heat transfer coefficients in the boiler from measured vaporization rates	In-house made differential model (including equations of: mass balance, heat balance, thermodynamic equilibrium and heat transfer)	*Vapor phase:* Virial equation coupled to the Hayden-O'Connell model *Liquid phase:* NRTL	*Solvent:* ethanol, water *Aroma compounds:* methanol, propan-1-ol, 2-methylpropan-1-ol, 3-methylbutan-1-ol; ethanal; ethanoic acid; ethyl ethanoate
Valderrama et al., 2012b *Whisky*	- Determination of the temporal evolution of aroma compounds concentrations in the distilled product, during the first distillation of a bi-distillation system in a classical industrial still. No comparison with experimental data.	ChemCAD	*Vapor phase:* Ideal gas *Liquid phase:* NRTL	*Solvent:* ethanol, water *Aroma compounds:* propan-1-ol, 2-methylpropan-1-ol, 3-methylbutan-1-ol; ethanal
Sacher et al., 2013 *Pear distillate*	- Estimation of the ethanol composition profile in the distillate as well as aroma compounds concentrations in different cuts of a lab-scale distillation unit (charentais alembic). Comparison with own experimental data.	In-house made differential model (including equations of: mass balance, heat balance, thermodynamic equilibrium and heat transfer)	*Vapor phase:* Ideal gas *Liquid phase:* UNIFAC	*Solvent:* ethanol, water *Aroma compounds:* 1,1-diethoxyethane; methanol, propan-1-ol, 2-methylpropan-1-ol, butan-1-ol, butan-2-ol, 2-methylbutan-1-ol, 3-methylbutan-1-ol, 2-phenylethan-1-ol; ethanal; methyl ethanoate, ethyl ethanoate, ethyl hexanoate, ethyl decanoate; furan-2-carbaldehyde
Esteban-Decloux et al., 2014 *Bitter orange distillate*	- Estimation and understanding of the temporal evolution of ethanol and aroma compounds concentrations in the distillate of an industrial still (composed of a boiler, a multistage column, and a total condenser). Comparison with own experimental data. - Improvement in the selection of the distillate cuts (considering the product quality, the recovery of ethanol in the heart fraction and the energy consumption) and understanding of the role of peels during distillation	BatchColumn	*Vapor phase:* Ideal gas *Liquid phase:* NRTL (binary ethanol–water), Henry's law (aroma compounds)	*Solvent:* ethanol, water *Aroma compounds:* α-Pinene, limonene, linalool, linalool oxide

component of the non-condensable streams and may modify the phase equilibria (Batista and Meirelles, 2011; Batista et al., 2012; Bastidas et al., 2012; Batista et al., 2013).

Concerning French spirits, to the best of our knowledge, no reports on simulation of the specific distillation units have been reported to date. In this context, the objective of the present work is to develop a methodology for the simulation of spirits distillation at steady state using ProSimPlus®, in order to improve the understanding of volatile aroma compounds behavior and provide scientific basis for the operation of the distillation units. The simulations were performed with the NRTL model, highly recommended for the thermodynamic modeling of hydroalcoholic mixtures at low pressures (Renon and Prausnitz, 1968; Valderrama et al., 2012a). Experimental distillation data for 66 volatile aroma compounds, having an impact on product quality, were acquired for this study. However, due to the lack of NTRL interaction parameters, only 32 species (including alcohols, carbonyl compounds, carboxylic acids and esters) were simulated.

The developed methodology was applied to the simulation of Armagnac distillation. This AOC spirit is produced by continuous distillation, in a tray column still known as *alambic armagnacais*. Double batch distillation is also performed in some plants, yet this method represents less than 5% of the production. By law, the distillation period has to be comprised between the end of the grapes harvest and the 31st march of the following year. The production region is located in southwestern France and covers more than 1000 ha divided in three areas: Bas-Armagnac, Tenareze and Haut Armagnac. In the column, the total number of trays is limited to 15, yet the number of concentration trays must not exceed two. The wash, wine in this case, is produced by fermentation of white grapes and its ethanol volume concentration at 20 °C (named ABV, alcohol by volume) must be between 7.5%v/v and 12.0%v/v (Bertrand, 2003; Decloux and Joulia, 2009; Ledauphin et al., 2010). As for fresh distillates, before ageing, their minimum ABV is fixed to 52.0%v/v and the maximum allowed, according to the last regulation is 72.4%v/v (JORF, 2015). The commercial product is obtained by dilution of aged distillates to a minimal ABV of 40%v/v. A classical composition analysis of commercial Armagnac after ageing is summarized in Table 2 (Bertrand, 2003).

In relation to the literature reports on alcoholic distillation, some novel contributions of this research can be highlighted:

- Development of a methodology for the systematic classification and understanding of volatile aroma compounds behavior in distillation. 16 'new' species are included, namely: (Z)-Hex-3-en-1-ol, octan-1-ol, decan-1-ol, dodecan-1-ol, tetradecan-1-ol, methanoic acid, butanoic acid, 2-methylpropanoic acid, 3-methylbutanoic acid, hexanoic acid, ethyl butanoate, 3-methylbutyl ethanoate, hexyl ethanoate, 2-phenylethyl ethanoate, ethyl octanoate and diethyl butane-1,4-dioate.
- Thermodynamic modeling using binary interaction parameters estimated from experimental data at high dilution, closer to the real conditions of spirits distillation. The methodology is developed in a review published by the authors (Puentes et al., 2018a, 2018b).
- Validation of simulation results of an industrial Armagnac unit, by comparison with experimental reconciled data.
- Focus on the influence of operating parameters such as extractions, thermal losses and reflux on distillate composition and energy consumption.

The paper is organized as follows: the development of the simulation methodology is described in Section 2. This includes the description of the process (2.1), experimental data acquisition (2.2) and reconciliation (2.3), as well as configuration of the simulation module in ProSimPlus® (2.4). In section 3, the simulation results of an industrial Armagnac unit are then presented and validated against experimental data. This validation is carried out on two levels (3.1): a first level, concerning exclusively the binary ethanol–water, and a second level that incorporates volatile aroma compounds. The behavior of volatile aroma compounds is classified in several groups by using a double criterion based on (i) their relative volatilities with respect to ethanol and water and (ii) the composition profiles in the distillation column. The work is concluded with the simulation of heads and tails extractions (3.2) and a detailed analysis of the influence of some operating parameters on the distillate composition and energy consumption (3.2). The impact on volatile aroma compounds is evaluated by subgroup, according to the classification established in the previous section.

2. Construction of the simulation module

The construction of a simulation module for spirits distillation at steady state is developed in this section. The simulation is focused on the understanding of volatile aroma compounds behavior.

In Fig. 1, a general schema of the framework is depicted. The module construction is comprised of the following phases:

- Selection and description of the distillation unit, aiming to identify the different circuits and their configuration.
- Data acquisition and reconciliation, for gathering of input data, and validation of mass and energy balances.
- Selection of a thermodynamic model, fundamental to correctly describe the phase equilibria and other volumetric properties.
- Configuration of the simulation module, which includes the selection of a distillation model, the introduction of input data and other specifications required to solve the modeling problem.

Two levels of simulation were considered: (i) a first level that only includes the two major components of the system, ethanol and water and (ii) a second level for the simulation of volatile aroma compounds distillation in the hydroalcoholic matrix. The aim of the fist level is to tune the global mass and energy balances using experimental reconciled data. Here, validation is based on coherence of the composition and flow profiles simulated in the column. Independent treatment from volatile aroma compounds is justified by the fact that the influence of these components on the mixture enthalpy, and therefore energy balance, can be neglected, as they are present at very low concentrations (Sacher et al., 2013). Concerning the second level, the aim is to validate the mass balance of volatile aroma compounds with experimental data and then to classify them according to the composition profiles simulated in the column.

Table 2 – Typical Armagnac composition after aging and dilution. Analysis of 15 representative samples. Adapted from (Bertrand, 2003).

Characteristic		Value	
		Average	Uncertainty
Ethanol volume concentration (ABV) at 20 °C	%v/v		
– Real		41.4	1.6
– Raw		40.1	2.3
Dry extract	gL^{-1}	4.5	3.5
Total acidity as ethanoic acid	gL^{-1}	153.9	57.6
Volatile acidity as ethanoic acid	mgL^{-1}	440.9	155.3
Total volatile compounds	mgL^{-1}	2823.9	346.1
Total alcohols	mgL^{-1}	2022.0	180.8
– methanol		194.6	45.1
– propan-1-ol		204.5	55.9
– 2-methylpropan-1-ol		432.6	78.7
– butan-1-ol		0.8	2.1
– butan-2-ol		2.1	3.5
– 2-methyl + 3-methylbutan-1-ol		1186.5	137.4
Total aldehydes as ethanal	mgL^{-1}	96.5	26.5
Total esters as ethyl ethanoate	mgL^{-1}	453.7	143.7
– ethyl ethanoate		315.9	99.4
– Furan-2-carbaldehyde	mgL^{-1}	5.0	1.2

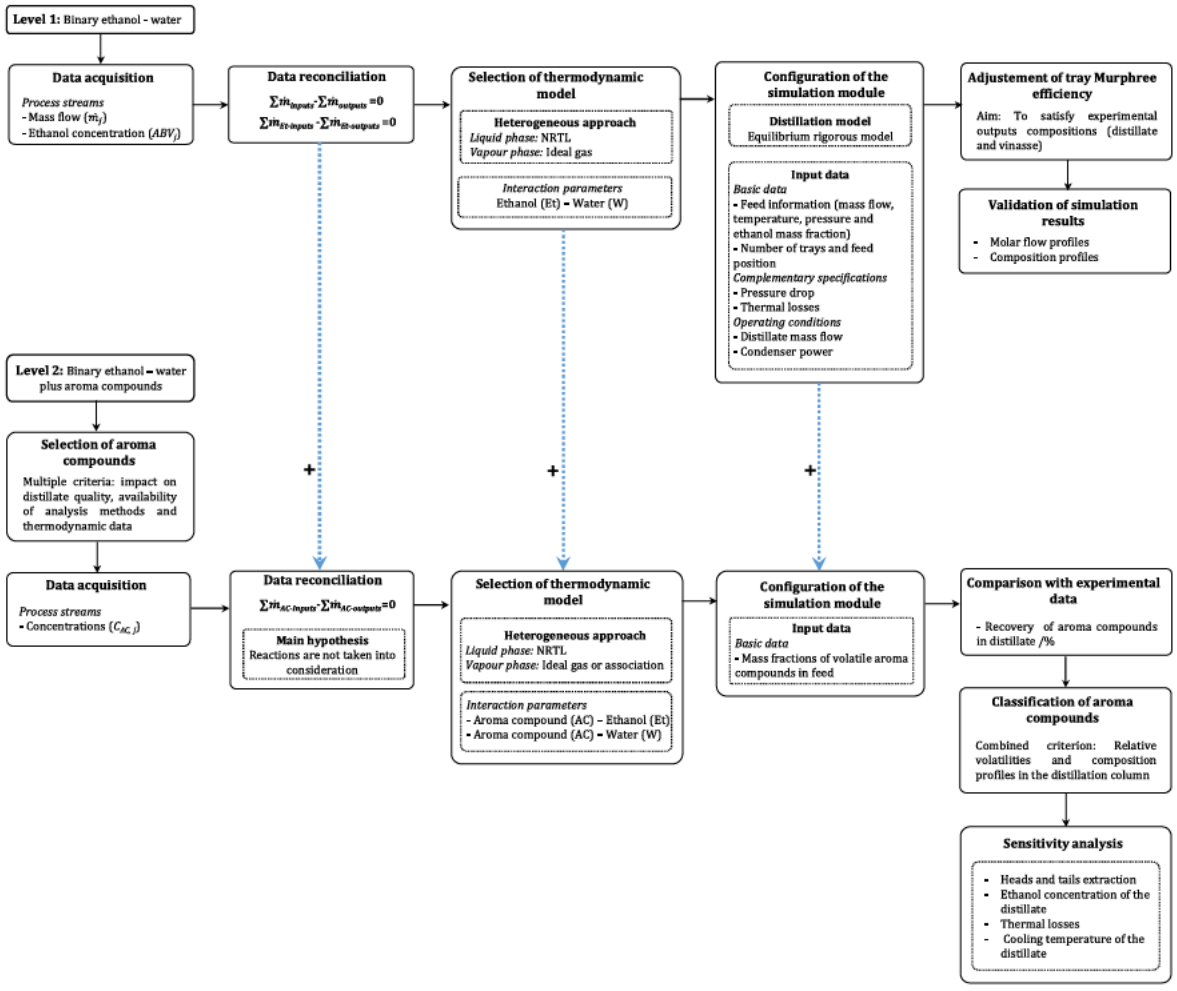

Fig. 1 – General methodology for the construction of the simulation module.

In this work, the methodology is applied to the simulation of a distillation unit for Armagnac production. However, it may be extended to other spirits. Further research on Calvados and comparison with Armagnac distillation will be reported in a companion paper.

It is important to mention that the simulation modules do not take into account the chemical reactions that may occur during the distillation. These phenomena are outside the scope of this work. Despite their influence on the generation of volatile compounds with an impact on product quality,

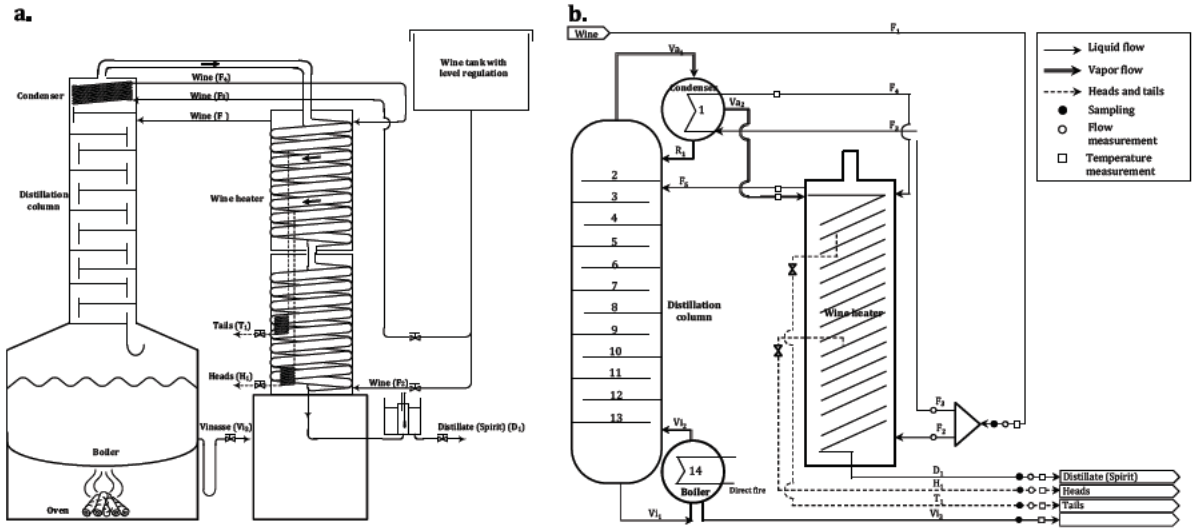

Fig. 2 – (a) Schema of the distillation unit for Armagnac production. (b) Corresponding process diagram.

information acquired in the spirits field is still very limited. Only a preliminary study in our research team has allowed the identification of a group of volatile compounds (including two esters, three aldehydes, 12 norisoprenoids, and three terpenes) formed during Cognac distillation, a process that comprises two successive 8 h batch cycles (Awad et al., 2017). However, to our knowledge, no analytical information about reactions kinetics in the conditions of spirits distillation have been published in the literature.

2.1. *Process description*

The installation selected for this study is an Armagnac distillation unit, located in the area of Armagnac Tenarèze. Its diary production capacity is about 20 hL of ethanol. The schema of the unit as well as the corresponding process flow diagram are presented in Fig. 2. It is a classical *alambic armagnac*is divided in two parts: (i) a tray column on top of a direct-fired boiler and (ii) a wine heater. All the elements are made of annealed electrical grade copper. The boiler is comprised of two compartments and operates with a natural gas burner. The column has 12 large bubble-cap trays, one for concentration, above the feed entry, and 11 for stripping. Inside, at top of the column, a coil heat exchanger works as partial condenser. The wine heater is an external coil heat exchanger used to preheat the wine while condensing and cooling the vapor distillate.

Wine (F_1) flows uninterruptedly by gravity from the load tank with a level regulation and is distributed between the wine heater (F_2) and the partial condenser (F_3) with a gate valve. The concrete load tank, fed with wine initially stored in tanks inside a cold warehouse, is placed in a closed room, next to the distillation room. In the wine heater, wine flows upwards in the external compartment and is heated by thermal transfer with the distillate vapor (Va_2) flowing in the coil. Then, it enters the column, above the first tray of the stripping section and flows through the trays towards the boiler. The vapor produced in the boiler bubbles through the stripping trays and then reaches the concentration tray, where it is mixed with a reflux stream (R_1) generated in the internal partial condenser. Thus, the mass and energy transfer between both phases lead to the concentration of ethanol and the extraction of volatile aroma compounds in the vapor phase. The liquid phase is in turn enriched with the less volatile species, including water.

The vapor distillate (Va_2) is drawn out of the column and transferred to the wine-heater where it flows down and condenses inside the coil. The wine stream fed to the internal partial condenser (F_3) is partially heated (F_4) and sent to the wine-heater to constitute with the stream F_2 the feed of the column (F_5). Finally, the fresh liquid distillate (D_1), is extracted and passes through an alcoholmeter, to measure its temperature and ethanol concentration. The bottom product or vinasse (Vi_3), stripped in ethanol, is continuously withdrawn through a siphon connected to the boiler.

Two accessory circuits in the wine-heater complete the installation. In the first one, for tails extraction (T_1), a fraction of the liquid flow is evacuated from the bottom of the second turn of the coil. The second one, for heads extraction (H_1), operates in the same way but is placed over one of the last turns of the coil before the cooling section, in order to extract a fraction of vapor phase. Tails are due to contain low volatility compounds that condense easily, while heads is expected to be rich in high volatility compounds that condense at the end of the thermal transfer. Currently, these circuits are not used in the process. However they were tested for simulation purposes in this work. Further details about this analysis are developed in Section 3.2.

Given that the distillation unit is not isolated from the environment, internal refluxes are generated by partial condensation of the vapor phase on the column wall. This phenomenon improves the separation capacity of the column and has therefore to be considered for a correct process modeling.

2.2. *Data acquisition*

An experimental campaign was carried out in order to characterize the nominal operation point of the installation and to stablish the corresponding mass and energy balances. The experiment took place in winter in a closed room, little exposed to exterior lighting. The information gathered play a double role of: (i) input data to saturate the freedom degrees of the simulation problem and (ii) validation data to check the reliability of the simulation results. The experimental campaign was performed during six hours, after stabiliza-

tion of the unit. Every hour, three variables were measured: temperatures, mass flows and distillate ethanol composition (Section 2.2.1). When possible, several instruments were used to verify the coherence of measurements. At the same time, some streams were sampled and representative global samples were constituted for each one at the end of the campaign, with the aim of quantifying ethanol and volatile aroma compounds composition (Section 2.2.2).

2.2.1. *Measurement of flows and temperatures*

A previous diagnostic of the installation evidenced a very important limitation in instrumentation. A reduced number of sensors were available before the experimental campaign: three thermocouples (2 placed in the column and one in the wine-heater), one alcohol thermometer for distillate control (D_1), and two flowmeters placed on the cold wine conduits (F_2 and F_3). Those instruments have not been calibrated for a long time and no online measurements or data recording were available.

In this context, new Pt100 probes Fluke-80PK-10 (Fluke, United States) were acquired to perform non-invasive measurements of temperature. They were placed on the following conduits: F_1, F_4 and Vi_3. Temperatures of wine (F_1) and distillate (D_1) were also measured by direct contact during the hourly sampling, using a Pt100 probe Checktemp1 (Hanna, country). In the case of wine, the relative deviations of the hourly and average temperatures (from 6 h measurements) using the Pt100 probe Fluke-80PK-10 and the Pt100 probe Chekctemp1 were about 9.8%, which can be explained by the different nature of the measurement (surface temperature vs. direct fluid contact). For distillate, the relative deviations between the hourly measurements using the Pt100 probe and the alcohol thermometer (both by direct contact with the liquid) vary between 0.0% and 5.3%, yet the deviation for the average temperature is only of 0.2%.

Thermal profiles of the column and wine-heater were studied by means of an infrared camera Ti9 (Fluke, United States). Some punctual temperatures were also measured with this device, including that of F_1, F_4, F_5 and Va_2. In the case of F_1 and F_4, the relative deviations of the hourly measurements with respect to the Pt100 values were lower than 7.1% for F_1 (deviation of the average temperature 3.4%) and lower than 4.2% for F_4 (deviation of the average temperature 0.2%).

In regard to vinasse temperature, the values measured on the conduit (hourly values between 98.2 °C and 100.6 °C, average value of 99.2 °C) were underestimated, considering that the major component of this stream is water and the boiler operates under a slight overpressure. This problem is due to the direct exposition of the vinasse conduit to the environment, whose temperature is around 20 °C. Thus, only simulation values for this variable will be considered to solve the energy balance.

Concerning stream flows, they were estimated by two ways: for wine (V_1), from the volume variation of the calibrated storage tank, and for distillate (D_1), from the filling time of a container, by means of a weighing-scale and a chronometer. In this latter case, every hourly measurement was made in triplicate, obtaining relative uncertainties lower than 0.7%. Due to evacuation and safety issues, the vinasse mass flow was not measured directly. It was determined from data reconciliation, as explained in Section 2.2.

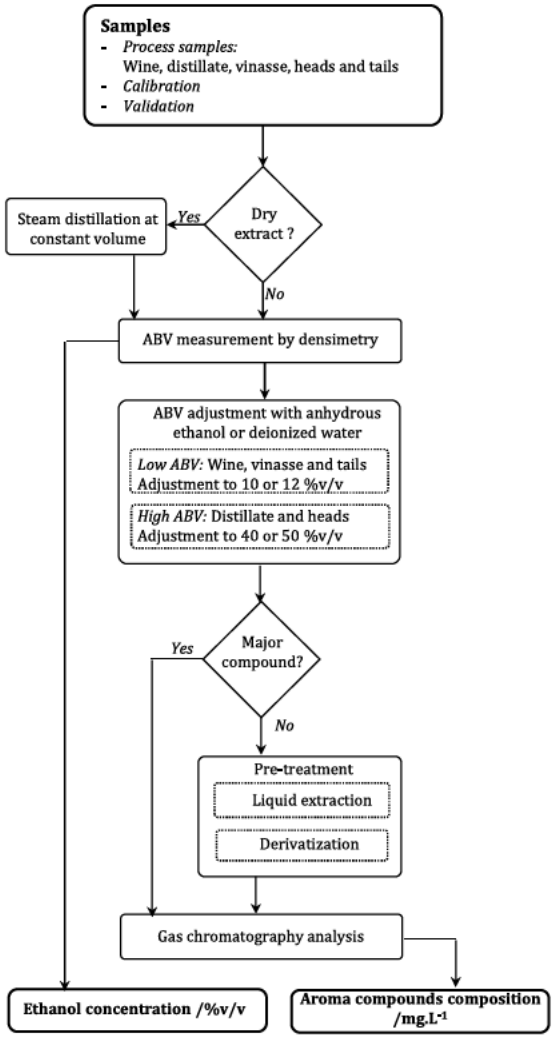

Fig. 3 – Methodology of chemical analysis of the process stream samples.

2.2.2. *Determination of ethanol and volatile aroma compounds compositions*

The composition of the process streams was determined by analysis of global samples obtained from mixing of 700 mL hourly samples. Three streams were sampled: feed wine (F_1), distillate (D_1) and vinasse (Vi_3).

The quantitative analysis were carried out at the UNGDA laboratory (*Union Nationale du Groupement de Distillateurs d'Alcool*, France), specialized in alcoholic beverages, bioethanol and neutral alcohol. The methodology, illustrated in Fig. 3, is based on OIV recommendations (OIV, 2014, 2016). The ABV of distillate was estimated from the mixture density at 20 °C, measured by electronic densitometry with a density meter DMA500 (Anton Paar, France), and then converted with the alcoholometric tables (OIML, 1975), integrated in the device calculator. For this estimation, the mixture is considered as a binary solution of ethanol and water, which leads to an error between 0.5% and 1.0%. The relative deviations between these measurements and those obtained in the production site, using a portable density meter DMA35 (Anton Paar, France) and an alcoholmeter, were lower than 0.1%,

For wine and vinasse samples, a previous step of steam distillation is necessary to eliminate dry extracts, solid material that modify the liquid density. The separation is carried out at constant volume, to avoid the alteration of ethanol content. The device is regularly controlled by distilling a sample of

known ABV. After five subsequent distillations, the ABV variation of the product should not exceed 0.1%, which corresponds to a maximal ethanol loss of 0.02% by measurement. For distillate samples, good agreement was obtained with respect to the measurements at the industrial plant, obtaining a relative deviation lower than 0.2%. For mass balance calculations, the selected values were those measured at UNGDA with the density meter DMA500, more precise than the DMA35.

In regard to volatile aroma compounds, the analysis was performed by gas chromatography coupled to detection by flame ionization (GC-FID). 66 volatile aroma compounds from seven chemical families were quantified: acetals, alcohols, carbonyl compounds, carboxylic acids, esters, furans and terpenes. Due to the mixture complexity, samples were separated in two groups and their ABV was adjusted to reference values: for the group of low ABV samples, the ABV was adjusted to 10 or 12%v/v and for the group of high ABV samples, the ABV was adjusted to 40 or 50%v/v. The adjustments were done with anhydrous ethanol or de-ionized water. This treatment aims at minimizing the matrix effects on the chemical analysis.

Then, according to the nature and concentration of volatile aroma compounds, three methods were applied:

- Direct injection: for analysis of major compounds, when no pretreatment is required.
- Liquid extraction: pretreatment to concentrate volatile aroma compounds present at very low concentrations, by using organic solvents.
- Derivatization: pretreatment to convert the analytes into products with more adapted properties for gas chromatography. In this work, derivatization was applied for the analysis of carboxylic acids, by transforming them into benzylic esters with very specific mass spectra and good response to flame ionization detectors.

Table 3 is a list of the volatile aroma compounds analyzed, classified by chemical family and analysis method. They are presented in an increasing order of molar mass. For further details about the different methods and analysis validation, the reader is directed to the Appendix Section.

2.2.3. *Data conversion*

For mass balance calculations, all the experimental compositions and flows must be expressed as temperature independent quantities. The average ABV values were converted into ethanol mass fractions by means of an empirical correlation established from literature data (OIML, 1975; Oudin, 1980):

$$x_{mEt,j} = C_1 ABV_j + C_2 ABV_j^2 + C_3 ABV_j^3 \quad (1)$$

here, $x_{mEt,j}$ is the ethanol mass fraction of the process stream j and ABV_j is the corresponding ABV. C_1–C_3 are coefficients determined by data regression. Their values are: $C_1 = 8.172 \times 10^{-3}$, $C_2 = -5.788 \times 10^{-6}$ and $C_3 = 2.332 \times 10^{-7}$.

Concerning the volatile aroma compounds, their mass fractions were obtained as follows:

$$x_{mAC,j} = \frac{C_{AC,j}}{10^6 \rho_{j-20}} \quad (2)$$

here, $x_{mAC,j}$ is the mass fraction of a volatile aroma compound AC in the process stream j, $C_{AC,j}$ is the corresponding concentration (mg L^{-1}) and ρ_{j-20} is the density (kg L^{-1}) of the process stream j at 20 °C, which corresponds to the analysis temperature.

Finally, water mass fractions ($x_{mW,j}$) were computed by difference, using the general formula:

$$x_{mW,j} = 1 - x_{mEt,j} - \sum_{AC=1}^{N} x_{mAC,j} \quad (3)$$

here, N (≤66) is the number of volatile aroma compounds quantified in the process stream j.

Regarding wine mass flow, this value was estimated from the experimental volume flow and mixture density at the average temperature of the stream (ρ_{j-T}). To simplify the calculation, this latter property was considered as a function of temperature (T in °C) and ethanol mass fraction ($x_{mEt,j}$). An empirical correlation for ethanol–water mixtures is available in the alcoholometric tables (OIML, 1975):

$$\rho_{j-T} = A_1 + \sum_{k=2}^{12} A_k x_{mEt,j}^{k-1} + \sum_{k=1}^{6} B_k (T-20)^k + \sum_{i=1}^{n} \sum_{k=1}^{m_i} C_{ik} x_{mEt,j}^{k-1} (T-20)^k \quad (4)$$

Here, A_k, B_k, C_{ik} are empirical coefficients estimated by regression of experimental density data. As previously stated, the influence of volatile aroma compounds can be neglected because of their low concentrations. In regard to dry extracts, even if they do have an influence on density, they will not be considered for two reasons: (i) the experimental values of ABV, used to compute ethanol mass fractions, were measured after their elimination from the hydro alcoholic matrix and (ii) they cannot be included in the simulation module, as the solution model only considers molecules in liquid or vapor phases. With respect to this latter argument, the direct measurement of a distillate mass flow remains coherent, because this stream do not contain dry extracts.

2.2.4. *Data reconciliation*

Direct application of the raw data set to validate mass balance is not possible for two reasons:

- The global mass balance is not redundant, as the experimental vinasse flow is unknown.
- For some volatile aroma compounds, the partial mass flow is bigger in distillate than in wine, which can be not only due to errors in the composition analysis, but also to chemical reactions that increase their output mass flow.

Data reconciliation is therefore required to generate a statistically coherent data set, from a minimal correction of the raw values, and to detect possible sensors faults and gross errors (Vrielynck, 2002; Sacher et al., 2013). The experimental values are corrected to satisfy some constraints as the conservation equations, mass balance in this case. This procedure can be formulated as an optimization problem of a system with m measured variables, in which the objective function to minimize is (Heyen and Arpentinier, 2017):

$$FO = \sum_{i=1}^{m} \left(\frac{V_{C,i} - V_{M,i}}{u_i} \right)^2 \quad (5)$$

Table 3 – Volatile aroma compounds quantified by gas chromatography.

Method	Family	Volatile aroma compound		No. CAS	MM/g mol^{-1}
		Common name	IUPAC name		
Direct injection-GC/FID	Acetals	Acetal	1,1-Diethoxyethane	105-57-7	118.2
	Alcohols	Methanol	Methanol	67-56-1	32.0
		2-Propenol	Prop-2-en-1-ol	107-18-6	58.1
		Propanol	Propan-1-ol	71-23-8	60.1
		Butanol	Butan-1-ol	71-36-3	74.1
		2-Butanol	Butan-2-ol	78-92-2	74.1
		Isobutanol	2-Methylpropan-1-ol	78-83-1	74.1
		2-Methylbutanol	2-Methylbutan-1-ol	137-32-6	88.1
		Isopentanol	3-Methylbutan-1-ol	123-51-3	88.1
	Carbonyl compounds	Acetaldehyde	Ethanal	75-07-0	44.1
	Esters	Ethyl acetate	Ethyl ethanoate	141-78-6	88.1
		Ethyl lactate	Ethyl 2-hydroxypropanoate	97-64-3	118.1
	Furans	Furfural	Furan-2-carbaldehyde	98-01-1	96.1
Liquid extraction-GC/FID	Acetals	1,1,3-Triethoxypropane	1,1,3-Triethoxypropane	7789-92-6	176.3
	Alcohols	Cis-3-hexenol	(Z)-Hex-3-en-1-ol	928-96-1	100.2
		Hexanol	Hexan-1-ol	111-27-3	102.2
		2-Heptanol	Heptan-2-ol	543-49-7	116.2
		2-Phenylethanol	2-Phenylethan-1-ol	60-12-8	122.2
		1-Octanol	Octan-1-ol	111-87-5	130.2
		1-Decanol	Decan-1-ol	112-30-1	158.3
		1-Dodecanol	Dodecan-1-ol	112-53-8	186.3
		1-Tetradecanol	Tetradecan-1-ol	112-72-1	214.4
Liquid extraction-GC/FID	Esters	Ethyl butyrate	Ethyl butanoate	105-54-4	116.2
		Isopentyl acetate	3-Methylbutyl ethanoate	123-92-2	130.2
		Cis-3-hexenyl acetate	(Z)-3-hexenyl ethanoate	3681-71-8	142.2
		Ethyl caproate	Ethyl hexanoate	123-66-0	144.2
		Hexyl acetate	Hexyl ethanoate	142-92-7	144.2
		2-Phenylethyl acetate	2-Phenylethyl ethanoate	103-45-7	164.2
		Ethyl caprylate	Ethyl octanoate	106-32-1	172.3
		Diethyl succinate	Diethyl butane-1,4-dioate	123-25-1	174.2
		Ethyl caprate	Ethyl decanoate	110-38-3	200.3
		Isopentyl caprylate	3-Methylbutyl octanoate	2035-99-6	214.3
		Ethyl laurate	Ethyl dodecanoate	106-33-2	228.4
		2-Phenylethyl caprylate	2-Phenylethyl octanoate	5457-70-5	248.4
		Ethyl myristiate	Ethyl tetradecanoate	124-06-1	256.4
		Isoamyl laurate	3-methylbutyl dodecanoate	6309-51-9	270.5
		Ethyl palmitate	Ethyl hexadecanoate	628-97-7	284.5
		Ethyl linoleate	Ethyl (9Z,12Z)-9,12-octadecadienoate	544-35-4	308.5
		Ethyl oleate	Ethyl (9Z)-octadec-9-enoate	111-62-6	310.5
		Ethyl stearate	Ethyl octadecanoate	111-61-5	312.5
	Furans	Ethyl 2-furoate	Ethyl furan-2-carboxylate	614-99-3	140.1
	Terpenes	Linalool	3,7-Dimethylocta-1,6-dien-3-ol	78-70-6	154.2
		α-terpineol	2-(4-Methyl-1-cyclohex-3-enyl)propan-2-ol	98-55-5	154.2
		Cis-Linalool oxyde	2-[(2R,5S)-5-ethenyl-5-methyloxolan-2-yl]propan-2-ol	5989-33-3	170.2
		Trans-Linalool oxyde	2-[(2S,5S)-5-ethenyl-5-methyloxolan-2-yl]propan-2-ol	34995-77-2	170.2
		Cis-Nerolidol	(Z)-3,7,11-Trimethyl-1,6,10-dodecatrien-3-ol	3790-78-1	222.4
		Trans-Nerolidol	(E)-3,7,11-Trimethyl-1,6,10-dodecatrien-3-ol	40716-66-3	222.4
Derivatization	Carboxylic acids	Formic acid	Methanoic acid	64-18-6	46.0
		Acetic acid	Ethanoic acid	64-19-7	60.1
		Propionic acid	Propanoic acid	79-09-4	74.1
		Butanoic acid	Butanoic acid	107-92-6	88.1
		Isobutanoic acid	2-Methylpropanoic acid	79-31-2	88.1
		Lactic acid	2-Hydroxypropanoic acid	50-21-5	90.1
		2-Methylbutanoic acid	2-Methylbutanoic acid	116-53-0	102.1
		Isovaleric acid	3-Methylbutanoic acid	503-74-2	102.1
		Caproic acid	Hexanoic acid	142-62-1	116.2
		Caprylic acid	Octanoic acid	124-07-2	144.2
		Capric acid	Decanoic acid	334-48-5	172.3
		Lauric acid	Dodecanoic acid	143-07-7	200.3
		Myristic acid	Tetradecanoic acid	544-63-8	228.4

– Table 3 (*Continued*)

Method	Family	Volatile aroma compound		No. CAS	MM/g mol^{-1}
		Common name	IUPAC name		
		Palmitoleic acid	(9Z)-Hexadec-9-enoic acid	373-49-9	254.4
		Palmitic acid	Hexadecanoic acid	57-10-3	256.4
		Linolenic acid	(9Z,12Z,15Z)-9,12,15-Octadecatrienoic acid	463-40-1	278.4
		Linoleic acid	(9Z,12Z)-9,12-Octadecadienoic acid	60-33-3	280.4
		Oleic acid	(9Z)-Octadec-9-enoic acid	112-80-1	282.5
		Stearic acid	Octadecanoic acid	57-11-4	284.5

where, $V_{M,i}$ is the measured value and $V_{C,i}$ the corrected value of the variable i. The standard deviation or absolute uncertainty, u_i, is included to apply the bigger corrections to the less accurate values.

The reconciliation was in a first step applied to calculate the vinasse mass flow and to simultaneously satisfy the ethanol mass balance, acting on total mass flows ($\dot{m}_j$) and ethanol mass fractions ($x_{mEt,j}$) (Esteban-Decloux et al., 2014). It is important to keep in mind that only the contributions of major components, ethanol and water, are considered to compute total mass flows in this step. The contribution of dry extracts and volatile aroma compounds are neglected.

In this context, the objective function depends on five variables ($\dot{m}_{F1}$, $x_{mEt,F1}$, $\dot{m}_{D1}$, $x_{mEt,D1}$, $x_{mEt,Vi3}$) and two constraints are taken into account:

$$\text{Global mass balance}: \quad \dot{m}_{F1}\text{-}\dot{m}_{D1}\text{-}\dot{m}_{Vi3}=0 \tag{6}$$

$$\text{Ethanol mass balance}: \quad \dot{m}_{F1}x_{mEt,F1}-\dot{m}_{D1}x_{mEt,D1}-\dot{m}_{Vi3}x_{mEt,Vi3}=0 \tag{7}$$

In a second step, the partial mass flow of volatile aroma compounds were corrected to verify the respective mass balance. For each volatile aroma compound, the constraint is written as:

$$\dot{m}_{F1}x_{mAC,F1}-\dot{m}_{D1}x_{mAC,D1}-\dot{m}_{Vi3}x_{mAC,Vi3}=0 \tag{8}$$

By fixing the total mass flows, a coherent set of mass fractions ($x_{mAC,j}$) can be calculated.

A supplementary constraint is defined when the concentration of a volatile aroma compound is lower than the quantification limit ($C_{AC,j} < QL_{AC}$). The measured value as well as its standard uncertainty are fixed at the respective quantification limit. The constraint is written in terms of partial mass flows by means of the Eq. (2). The following expression is obtained:

$$\dot{m}_{AC,j}-\frac{QL_{AC}}{10^6\rho_{j-20}}\dot{m}_j<0 \tag{9}$$

The sets of measured and reconciled values, including mass flows and compositions of wine, distillate, and vinasse are presented in Table 4.

The ethanol concentrations are reported as ABV values (%v/v) and mass fractions. Concerning aroma compounds, composition values are reported as volume concentrations (mg L^{-1}) to facilitate their reading and interpretation.

According to this synthesis, the reconciled values of mass flows and ethanol concentrations are in good agreement with the measurements, as the relative deviations are lower than 4.0%.

In regard to volatile aroma compounds, except for methanoic acid and ethanoic acid, high deviations are mainly associated to the species at very low concentrations. Two factors might justify this result: analysis errors and occurrence of chemical reactions. On one hand, although gas chromatography is a technique adapted to the system tackled in this work, aspects such as matrix complexity, sample preparation and overlapping spectra may have a negative impact on quantification. On the other hand, since the measured mass flows were reconciled without taking into account mass generation or consumption, the correction applied for species that were actually involved in chemical reactions may be very important to satisfy the simplified mass constraints.

Despite these problems, from a general point of view, the relative deviations are acceptable, with overall values for each process stream between 10% and 37%. Moreover, as the lowest deviations are associated to distillate (10%), product of interest, the results from reconciliation can be considered as satisfactory for the simulation purposes of this work.

2.3. *Simulation procedure with ProSimPlus®*

2.3.1. *Thermodynamic model*

A heterogeneous approach, also known as gamma-phi method, was selected to model phase equilibria of the investigated system. Since the distillation unit operates at atmospheric pressure, the vapor phase can be considered as an ideal gas, except for the case of carboxylic acids, which can be associated as dimers due to strong hydrogen bonds (Allen and Caldin, 1953; Vawdrey et al., 2004). For these compounds, a correction term is included (Detcheberry et al., 2016). The corresponding model is available in Simulis Thermodynamics®, suite for phase equilibria and properties calculations of ProSimPlus®.

The non-ideality of the liquid phases was represented by the NRTL model (Renon and Prausnitz, 1968), used in most simulation works reported in literature on alcohol distillation and recommended by different authors (Valderrama and Faúndez, 2003; Faúndez and Valderrama, 2004, 2009; Faúndez et al., 2006; Athès et al., 2008; Valderrama et al., 2012a). In this model, the binary interaction parameters required to compute the activity coefficients are determined from phase equilibria data. The non-randomness parameter was set at $\alpha = 0.3$ for all binaries. For binary ethanol–water, the parameters used in this work were those reported by (Kadir, 2009), validated against different sets of literature data (Arce et al., 1996; Yang and Wang, 2002; Kamihama et al., 2012; Lai et al., 2014). The values are presented in Table 5.

Concerning the volatile aroma compounds, the parameters were estimated from experimental data at high dilution, closer to the real conditions of spirits distillation. Only the interac-

Table 4 – Measured and reconciled values for mass flows and compositions.

Process stream	Feed – F1			Distillate – D_1			Vinasses – Vi_3		
Variable	Measured value		Reconciled value	Measured value		Reconciled value	Measured value		Reconciled value
	Average	Uncertainty		Average	Uncertainty		Average	Uncertainty	
Mass flow/kg.h^{-1}	856.3	9.8	866.2	126.0	1.5	127.4	–	–	738.7
Ethanol concentration/%v/v	10.8	0.1	10.8	64.8	0.3	64.9	0.33	0.02	0.34
Ethanol mass fraction	0.086	0.001	0.086	0.569	0.003	0.570	0.0027	0.0002	0.0028
Volatile aroma compounds concentrations/mg L^{-1}									
Volatile aroma compound									
1,1-Diethoxyethane	–	–	–	<6.5	<6.5	6.5	–	–	–
1,1,3-Triethoxypropane	<0.1	<0.1	0.1	<0.1	<0.1	0.1	<0.1	<0.1	0.1
Methanol	40.7	1.2	41.0	194.6	0.0	194.6	12.7	0.6	11.1
Prop-2-en-1-ol	–	–	–	<6.5	<6.5	6.5	–	–	–
Propan-1-ol	17.3	1.2	17.9	110.3	0.0	110.3	<5.0	<5.0	0.0
Butan-1-ol	<5.0	<5.0	5.0	<6.5	<6.5	6.5	<5.0	<5.0	4.7
Butan-2-ol	<5.0	<5.0	5.0	<6.5	<6.5	6.5	<5.0	<5.0	4.7
2-Methylpropan-1-ol	135.0	1.0	136.8	843.2	0.0	843.2	<5.0	<5.0	0.0
2-Methylbutan-1-ol	74.7	1.2	75.8	470.2	4.6	470.2	<5.0	<5.0	0.0
3-Methylbutan-1-ol	304.0	2.0	305.1	1903.6	22.9	1903.6	<5.0	<5.0	0.0
(Z)-Hex-3-en-1-ol	0.2	0.0	0.4	1.7	0.0	1.7	<0.1	<0.1	0.1
Hexan-1-ol	1.6	0.0	1.6	10.8	0.0	10.8	<0.1	<0.1	0.0
Heptan-2-ol	<0.1	<0.1	0.1	<0.1	<0.1	0.1	<0.1	<0.1	0.1
2-Phenylethan-1-ol	31.5	0.5	29.8	17.3	0.1	17.3	29.4	0.8	32.0
Octan-1-ol	<0.1	<0.1	0.1	0.2	0.0	0.2	<0.1	<0.1	0.1
Decan-1-ol	<0.1	<0.1	0.1	0.1	0.1	0.1	<0.1	<0.1	0.1
Dodecan-1-ol	<0.1	<0.1	0.1	<0.1	<0.1	0.1	<0.1	<0.1	0.1
Tetradecan-1-ol	<0.1	<0.1	0.1	0.2	0.0	0.2	<0.1	<0.1	0.1
Ethanal	<10.0	<10.0	9.4	<6.5	< 6.5	6.5	<10.0	<10.0	9.9
Methanoic acid	38.3	44.9	32.7	4.8	0.8	4.8	11.0	2.6	37.7
Ethanoic acid	229.7	156.9	120.3	<0.1	<0.1	0.1	78.0	20.1	142.4
Propanoic acid	8.7	10.7	1.2	0.7	0.1	0.7	1.3	0.6	1.3
Butanoic acid	36.0	56.3	1.6	1.2	0.0	1.2	1.7	0.6	1.7
2-Methylpropanoic acid	1.7	1.2	1.7	1.2	0.0	1.2	4.3	3.2	1.7
2-Hydroxypropanoic acid	–	–	–	9.8	3.7	9.8	–	–	–
2-Methylbutanoic acid	7.3	11.0	0.9	0.5	0.1	0.5	<1.0	<1.0	1.0
3-Methylbutanoic acid	<1.0	<1.0	0.9	0.6	0.0	0.6	<1.0	<1.0	1.0
Hexanoic acid	23.0	19.3	3.2	6.0	0.0	6.0	2.7	1.5	2.6
Octanoic acid	23.7	16.6	4.6	23.1	0.1	23.1	<1.0	<1.0	1.0
Decanoic acid	3.7	4.6	2.8	12.0	0.0	12.0	<1.0	<1.0	1.0
Dodecanoic acid	< 1.0	<1.0	1.0	3.2	0.0	3.2	<1.0	<1.0	0.6
Tetradecanoic acid	–	–	–	8.5	2.1	8.5	–	–	–
(9Z)-Hexadec-9-enoic acid	–	–	–	<1.0	<1.0	1.0	–	–	–
Hexadecanoic acid	–	–	–	2.0	0.0	2.0	–	–	–
(9Z,12Z,15Z)-9,12,15-Octadecatrienoic acid	–	–	–	<1.0	<1.0	1.0	–	–	–

– Table 4 (*Continued*)

Process stream	Feed – F1			Distillate – D_1			Vinasses – Vi_3		
Variable	Measured value		Reconciled value	Measured value		Reconciled value	Measured value		Reconciled value
	Average	Uncertainty		Average	Uncertainty		Average	Uncertainty	
(9Z,12Z)-9,12-Octadecadienoic acid	–	–	–	<1.0	<1.0	1.0	–	–	–
(9Z)-Octadec-9-enoic acid	–	–	–	<1.0	<1.0	1.0	–	–	–
Octadecanoic acid	–	–	–	<1.0	<1.0	1.0	–	–	–
Ethyl ethanoate	17.0	1.7	18.9	116.7	0.0	116.7	<10.0	<10.0	0.0
Ethyl butanoate	0.3	0.0	0.4	1.5	0.1	2.1	0.1	0.1	0.1
Ethyl 2-hydroxypropanoate	–	–	–	45.4	0.0	0.0	–	–	–
3-Methylbutyl ethanoate	0.6	0.0	0.7	3.5	0.1	4.1	<0.1	<0.1	0.1
(Z)-3-hexenyl ethanoate	<0.1	<0.1	0.1	<0.1	<0.1	0.1	<0.1	<0.1	0.1
Ethyl hexanoate	0.7	0.0	0.9	5.0	0.0	5.2	0.1	0.1	0.1
Hexyl ethanoate	<0.1	<0.1	0.1	0.1	0.0	0.1	<0.1	<0.1	0.1
2-Phenylethyl ethanoate	<0.1	<0.1	0.1	<0.1	<0.1	0.1	<0.1	<0.1	0.1
Ethyl octanoate	0.9	0.1	1.8	11.6	0.0	11.4	0.1	0.1	0.0
Diethyl butane-1,4-dioate	0.2	0.1	0.1	<0.2	<0.2	0.2	0.1	0.1	0.1
Ethyl decanoate	0.2	0.0	1.5	15.3	0.0	9.0	0.1	0.1	0.0
3-Methylbutyl octanoate	<0.1	<0.1	0.1	0.6	0.0	0.6	0.1	0.1	0.0
Ethyl dodecanoate	<0.1	<0.1	0.1	9.4	0.0	0.6	0.1	0.1	0.0
2-Phenylethyl octanoate	<0.1	<0.1	0.1	<.1	<0.1	0.1	0.1	0.1	0.1
Ethyl tetradecanoate	<0.1	<0.1	0.1	3.5	0.1	0.6	0.1	0.1	0.0
3-Methylbutyl dodecanoate	0.1	0.0	0.2	0.5	0.0	1.0	0.1	0.1	0.1
Ethyl hexadecanoate	<0.1	<0.1	0.1	3.6	0.1	0.6	0.1	0.1	0.0
Ethyl (9Z,12Z)-9,12-octadecadienoate	<0.1	<0.1	0.1	2.2	0.1	0.6	0.1	0.1	0.0
Ethyl (9Z)-octadec-9-enoate	<0.1	<0.1	0.1	0.3	0.0	0.3	0.1	0.1	0.1
Ethyl octadecanoate	<0.1	<0.1	0.1	0.2	0.0	0.2	0.1	0.1	0.1
Furan-2-carbaldehyde	–	–	–	<6.5	<6.5	6.5	–	–	–
Ethyl 2-furoate	<0.1	<0.1	0.1	<0.1	<0.1	0.1	<0.1	<0.1	0.1
3,7-Dimethylocta-1,6-dien-3-ol	<0.1	<0.1	0.1	0.2	0.0	0.2	<0.1	<0.1	0.1
2-(4-Methyl-1-cyclohex-3-enyl)propan-2-ol	<0.1	<0.1	0.1	0.1	0.0	0.1	<0.1	<0.1	0.1
2-[(2R,5S)-5-Ethenyl-5-methyloxolan-2-yl]propan-2-ol	<0.1	<0.1	0.1	<0.1	<0.1	0.1	<0.1	<0.1	0.1
2-[(2S,5S)-5-Ethenyl-5-methyloxolan-2-yl]propan-2-ol	<0.1	<0.1	0.1	<0.1	<0.1	0.1	<0.1	<0.1	0.1
(Z)-3,7,11-Trimethyl-1,6,10-dodecatrien-3-ol	<0.1	<0.1	0.1	<0.1	<0.1	0.1	<0.1	<0.1	0.1
(E)-3,7,11-Trimethyl-1,6,10-dodecatrien-3-ol	<0.1	<0.1	0.1	0.2	0.0	0.2	<0.1	<0.1	0.1

Table 5 – Interaction parameters of the NRTL model for the binary ethanol (2) – water (3). Taken from (Kadir, 2009).

Solvent.	i	j	A_{ij}^0/cal mol^{-1}	A_{ji}^0/cal mol^{-1}	A_{ij}^T/cal mol^{-1} K^{-1}	A_{ij}^T/cal mol^{-1} K^{-1}
Ethanol – Water	2	3	34.02	850.12	−1.80	5.65

tions volatile aroma compound–ethanol and volatile aroma compound–water were considered. Besides, the temperature dependence of the interaction parameters was neglected ($A_{ij}^T = 0$, $A_{ji}^T = 0$), as the temperature interval is fixed by the composition of the solvent ethanol–water in boiling conditions. Further details on the estimation and validation methodology are presented in a companion paper (Puentes et al., 2018a). Due to the lack of equilibrium data, only parameters for 26 compounds concerned in this work were obtained. Parameters for 1, 1-diethoxyethane, 2-hydroxypropanoic acid and furan-2-carbaldehyde were also available, but these compounds were not simulated because their compositions in wine and vinasse were not measured. Six supplementary compounds (octan-1-ol, decan-1-ol, dodecan-1-ol, tetradecan-1-ol, ethyl butanoate and hexyl ethanoate) were then added to complete the group of 32 compounds simulated. In this case, the interaction parameters were estimated from vapor–liquid equilibria predictions, using the UNIFAC model version 1993 (Gmehling et al., 1993).

2.3.2. *Configuration of the simulation module*

The flowsheet for static simulations was built in ProSimPlus® using the standard modules of distillation, heat transfer and mixing. The distillation was modeled using the rigorous equilibrium approach, based on the MESH equations (Kister, 1992). As previously stated, the simulation module must take into account the thermal losses, as the column, copper-made, is not isolated from the environment.

For the first simulation level, in which only the binary ethanol–water was considered, input data includes:

- Column configuration: unit of 14 stages, including 12 trays, 1 partial condenser and 1 boiler.
- Feed: Wine ($\dot{m}_{F5} = \dot{m}_{F1} = 866.1\,kg\,h^{-1}$; $T_{F5} = 76.4\,°C$; $P_{F5} = P_{F1} = 101.3\,kPa$; $x_{mEt,F5} = x_{mEt,F1} = 0.086$) introduced at stage 3 (numbered from top to bottom).
- Temperature data set: for most process streams (F_1, F_2, F_3, F_4, F_5 and D_1) temperatures were fixed at the experimental raw values. For the others streams (R_1, Va_1, Va_2, Vi_1, Vi_2 and Vi_3) the values are estimated by simulation.
- Operating conditions: two operating conditions are required to saturate the two degrees of freedom of the model, the feed being fixed, and then to solve the simulation problem. Physically these two degrees of freedom correspond to the control variables of the distillation unit: heat duty and reflux, via the ratio between F_2 and F_3. Taking into account the reliability of the measurements, the distillate mass flow and the condensation power were selected. The first was measured in triplicate every hour during six hours, obtaining a reconciled value of 127.4 kg h^{-1} with relative incertitude of 1.2%. The second can be estimated from mass flow and temperature measurements, according to the following equation:

$$\dot{Q}_C = c_{P,F3}\dot{m}_{F3}(T_{F4} - T_{F3}) \quad (10)$$

Here, $c_{P,F3}$ is the specific heat at constant pressure (computed to 4.1 kJ kg^{-1} K^{-1} with Simulis Thermodynamic®), the mass flow of the stream F_3 (estimated from a correction of the flowmeter value to 187.1 kg h^{-1}), and T_{F4} and T_{F3} the temperatures after and before condensation (measured values of 66.2 °C and 13.1 °C, respectively). The average power obtained was 11.6 kW, considering the contribution of 0.4 kW for thermal losses.

The condensation power was preferred to the heat power in the boiler because an accurate estimation of this latter requires the knowledge of supplementary data (such as temperature and composition of fumes, thermal losses) that were not available during the experimental campaign.

- Complementary specifications: column top pressure fixed at 101.3 kPa and pressure drop of 0.4 kPa by tray. Thermal losses ($\dot{Q}_{TL}$) were estimated by considering two transfer mechanisms: natural convection of air and radiation of copper:

$$\dot{Q}_{TL} = hS(T_S - T_\infty) + \varepsilon\sigma S{T_S}^4 \quad (11)$$

In this equation, h is an average convective heat transfer coefficient (estimated to 6.0 W m^{-2} K^{-1} from empirical correlations for vertical cylinders, proposed by Day (2012), S the transfer surface (total column surface estimated to 5.0 m^2), T_S the average temperature of the column surface (estimated to 94 °C), T_∞ the air temperature (measured value of 20 °C), the emissivity of polished copper (about 0.04, according to Çengel, 2007) and σ the Boltzmann Constant (5.7×10^{-8} W m^{-2} K^{-4}). Thus, considering the column geometry and the distance between trays, two average losses were fixed: 0.2 kW in each tray (stages 2–13) and 0.4 kW at stage 1, where the internal condenser is located. The thermal losses in the boiler are taken into account indirectly, as the effective heat power is calculated by the simulator to verify the fixed values of quantity (flow) and quality (ethanol concentration) of the distillate.

Finally, the Murphree efficiencies ($\tilde{E}$) in the stripping section were adjusted between 0.5 and 1.0, in order to verify the reconciled ethanol mass fractions of the outputs streams. The relationship between both parameters is shown in Fig. 4. According to this result, the Murphree efficiency was fixed at 0.68. For the concentration plate, the efficiency was fixed at a lower value, 0.58, considering that the reflux flow is low (about 19.8 kg h^{-1}). This may favor preferential flow pathways, reducing the contact with the vapor phase and therefore the concentration efficiency.

Concerning the second simulation level, all the parameters tuned in the first simulation level are maintained and the 32 volatile aroma compounds are added into the feed at the reconciled mass compositions.

3. Analysis of simulation results

This section is focused on the analysis of simulation results for the unit of Armagnac distillation. The first step consists in the representation of the nominal operation point to validate the simulation module. The validation is performed by comparison between experimental and simulation data in two levels: for the first level, binary ethanol – water, it is based on the coherence of the simulated composition and molar flow profiles, and for the second one, multicomponent volatile aroma

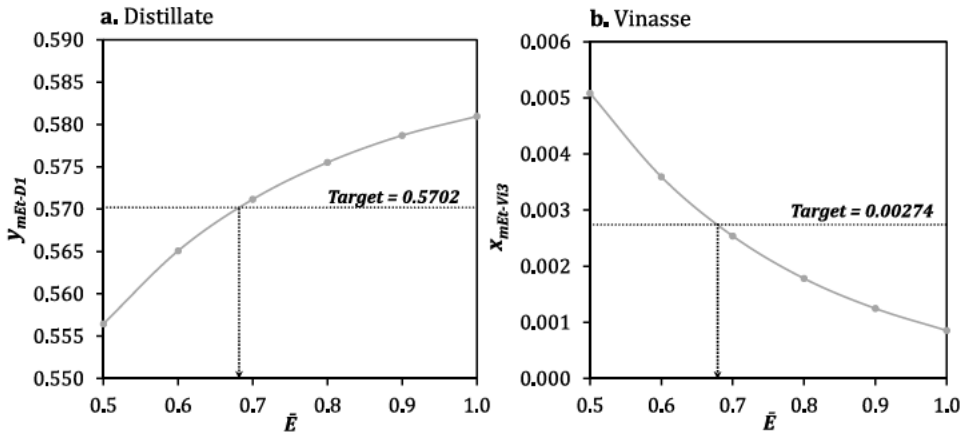

Fig. 4 – Adjustment of the Murphree tray efficiency of the stripping section to verify the ethanol outputs composition.

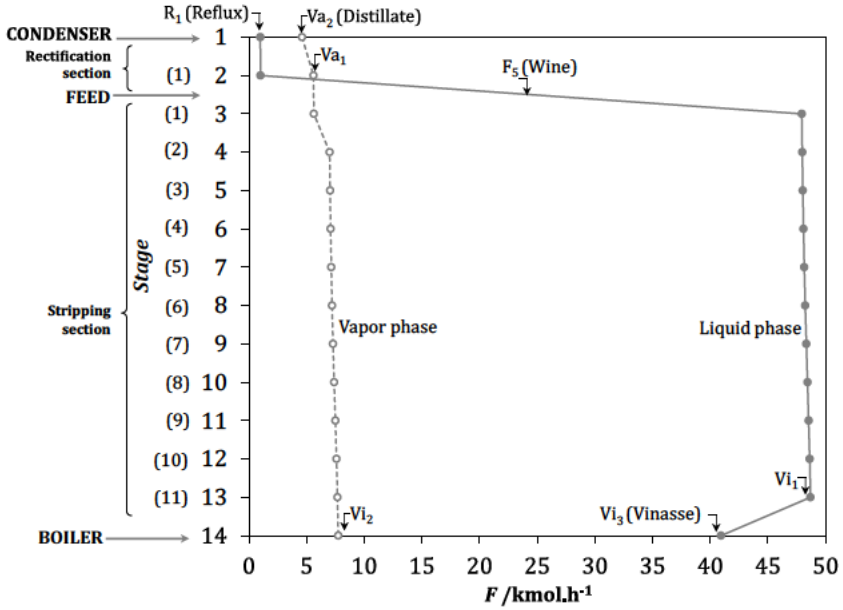

Fig. 5 – Molar flow profiles through the distillation column at the nominal operation point.

compounds – ethanol–water mixture, by comparison between experimental and simulated data of partial mass flows and mass recovery from feed to distillate.

Given that the main objective of the study is to better understand the behavior of volatile aroma compounds and process performance, a systematic classification is then proposed, according to their relative volatilities and their composition profiles in the column. Afterwards a simulation of the circuits of heads and tails extractions is proposed and validated against experimental data collected during the experimental campaign. Finally, the influence of some operating parameters (including ethanol concentration in the distillate, thermal losses and distillate temperature after condensation) is evaluated with respect to the composition of volatile aroma compounds in the distillate and energy consumption in the boiler. Analysis on the influence of ethanol concentration and thermal losses is based on different simulations, while for the distillate temperature, only theoretical calculations are considered.

3.1. *Validation of the nominal operation point*

3.1.1. *Level 1: Binary ethanol–water*

In the first level of simulation, the global and ethanol mass balances were tuned to the experimental reconciled values. The ethanol recovery in the distillate is 97.32% of the amount fed into the column, which corresponds to a maximum concentration of 2700 mg/kg in the vinasse, acceptable for Armagnac production. The reflux ratio calculated by simulation is 0.22, a ratio that justifies the relatively low ABV of distillate, 64.9%v/v. This value is within the appropriate concentration range stablished by legislation (52.0%v/v and 72.4%v/v).

The molar flow profile of liquid and vapor phases in the column is depicted in Fig. 5. The increase of liquid mass flow between stages 2 and 3 corresponds to the introduction of wine. Following the direction of flow (upwards for vapor and downwards for liquid), the simulation predicts a continuous decrease of the vapor flow while the liquid one (before the boiler) increases at the same rate. This phenomenon corresponds to the internal refluxes (partial condensation of the vapor phase) due to thermal losses through the column on each tray. The more pronounced reduction of vapor flow between stages 4 and 3 is associated with a supplementary condensation due to wine feed, whose temperature, despite being preheated, is lower than the temperature at stage 3.

The ethanol concentration profile is presented in Fig. 6. Although the absolute variation of liquid ethanol concentration is less pronounced than that of the vapor phase, the corresponding concentration factor in the liquid phase (defined as the ratio of ethanol concentration between the

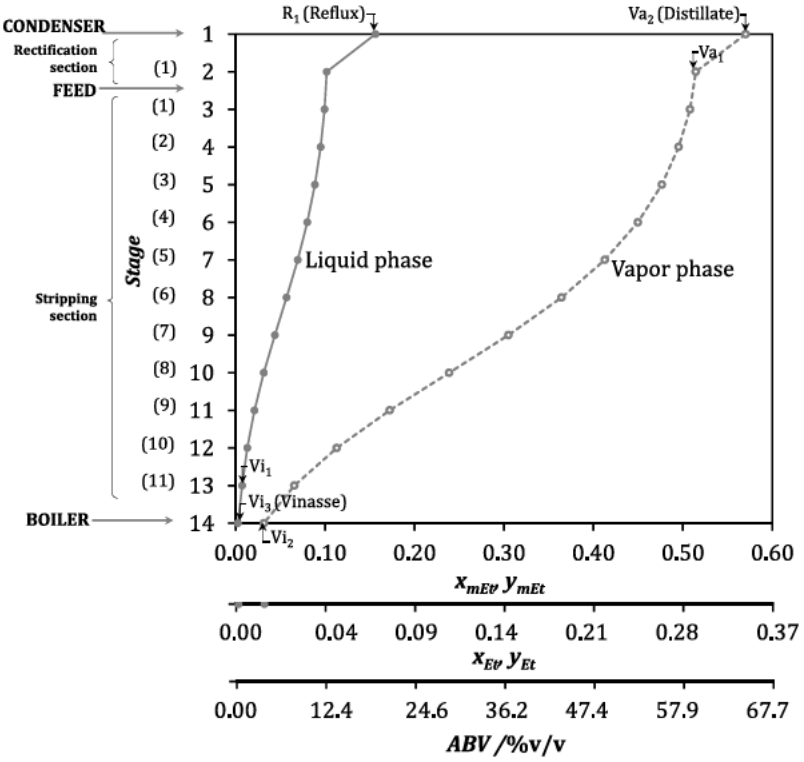

Fig. 6 – Ethanol composition profiles through the distillation column at the nominal operation point (in mass fraction, molar fraction and ABV).

reflux R_1 and vinasse Vi_3) is about 64 in molar basis (57 in volume), a value considerably higher than the concentration factor in the vapor phase (concentration ratio between distillate Va_2 and Vi_2), equivalent to 27 in molar basis (16 in volume). This result is coherent with the column configuration and indicates that the column plays a preponderant role of ethanol stripping.

The composition profiles here simulated are very different from the profiles in other alcohol distillation units, including those of neutral alcohol and bioethanol production (Decloux and Coustel, 2005; Batista et al., 2012, 2013; Esteban-Decloux et al., 2014), where the distillate has an important ethanol concentration and, as a result, the liquid and vapor compositions at top are very close. Three main factors explain this difference: (i) the number of rectification trays is reduced (the Armagnac units are conceived as stripping columns with only two rectification trays, while in bioethanol or neutral alcohol units, this number is around 40–50), (ii) the distillate is withdrawn as a vapor, since the internal coil operates as a partial condenser, and (iii) the internal reflux generated by the partial condenser in the Armagnac unit is very low (0.22).

In matters of energy balance, the net heat power in the boiler calculated by simulation is 88.5 kW. This value is coherent with those reported for other Armagnac units with similar production capacity (Marty and Cluzeau, 2010). The heat exchanged in the wine heater was computed by two ways: regarding the cold fluid (F_3), which is preheated to 76.4 °C, and regarding the hot fluid (Va_2), condensed then cooled to 18.8 °C. The average value obtained is 55.2 kW and the relative deviation between the estimations is 15.6%. This difference results from the combined effect of different error sources, including: (i) the estimation of wine enthalpy flow without considering the contribution of solid materials, present in the real feed and (ii) the temperature of streams, most of which were indirectly measured from surface temperatures of a conductor material. Nevertheless, the current deviation in the wine heater energy balance should not affect the analysis of volatile aroma compounds behavior, as the distillation column, where separation takes place, is well represented.

A final recapitulation of average mass flows, temperatures and ethanol compositions for the distillation unit is presented in Table 6.

3.1.2. *Level 2: Binary ethanol–water plus volatile aroma compounds*

3.1.2.1. Comparison between experimental data and simulation. A comparison between experimental and simulation data for the group of 32 volatile aroma compounds is presented in Table 7. This synthesis reveals that the consistency of concentrations is variable. For some major (including propan-1-ol, 2-methylpropan-1-ol, 2-methylbutan-1-ol, 3-methylbutan-1-ol and ethyl ethanoate) and minor species (hexan-1-ol, methanoic acid, 2-methylpropanoic acid, ethyl octanoate and ethyl decanoate) the deviations are very low in both distillate and vinasse. For another group of compounds (methanol, 2-phenylethan-1-ol, propanoic acid, butanoic acid, 3-methylbutanoic acid, hexanoic acid, octanoic acid, diethyl butane-1,4-dioate), the deviations become more important but the experimental and simulated values have the same orders of magnitude, even in the case of very low concentrations, around 0.1 mg L^{-1}. For compounds such as (Z)-hex-3-en-1-ol, ethyl butanoate, 3-methylbutyl ethanoate and ethyl hexanoate, although deviations of concentrations in vinasse could be considered high, as simulation predicts zero mass flows, the deviations for distillate are rather low. For ethanoic acid, the simulation prediction is close to the experimental value in vinasse, but in distillate the deviation is rather high, considering that the experimental concentration is about 0. For the remaining volatile aroma compounds (butan-1-ol, octan-1-ol, decan-1-ol, dodecan-1-ol, tetradecan-1-ol, ethanal, hexyl

Table 6 – Synthesis of the main properties of all the process streams in the distillation unit. Exp: Raw (non-reconciled) experimental value. R Exp: Reconciled experimental value. Sim: Simulation value.

Process stream	Mass flow/kg h^{-1}		Ethanol mass fraction		Temperature/°C	
	Value	Source	Value	Source	Value	Source
F_1	866.2	R Exp	0.086	R Exp	13.1	Exp
F_2	678.8	R Exp	0.086	R Exp	13.1	Exp
F_3	187.4	Exp	0.086	R Exp	13.1	Exp
F_4	187.4	Exp	0.086	R Exp	66.2	Exp
F_5	866.2	R Exp	0.086	R Exp	76.4	Exp
Va_1	147.3	Sim	0.514	Sim	91.6	Sim
Va_2	127.4	R Exp	0.570	R Exp	88.8	Sim
D_1	127.4	R Exp	0.570	R Exp	18.8	Exp
R_1	19.8	Sim	0.156	Sim	88.8	Sim
Vi_1	881.3	Sim	0.007	Sim	100.4	Sim
Vi_2	142.5	Sim	0.032	Sim	101.1	Sim
Vi_3	738.7	R Exp	0.003	R Exp	101.1	Sim

Table 7 – Experimental and simulated data of mass flow and composition in the main process streams.

Process stream	Feed – F_1	Distillate – D_1		Vinasse – Vi_3	
Variable	Simulation = Experimental	Experimental	Simulation	Experimental	Simulation
Mass flow/kg h^{-1}	866.2	127.4	127.4	738.7	738.7
Partial mass flows/kg h^{-1}					
Ethanol	74.7	72.7	72.7	2.0	2.0
Water	790.8	54.2	54.2	736.5	736.6
Concentration/mg L^{-1}					
Volatile aroma compounds					
Methanol	41.0	194.6	171.1	11.1	15.6
Propan-1-ol	17.9	110.3	109.9	0.0	0.1
Butan-1-ol	5.0	6.5	30.8	4.7	0.0
2-Methylpropan-1-ol	136.8	843.2	843.0	0.0	0.0
2-Methylbutan-1-ol	75.8	470.2	467.3	0.0	0.0
3-Methylbutan-1-ol	305.1	1903.6	1880.1	0.0	0.0
(Z)-Hex-3-en-1-ol	0.4	1.7	2.4	0.1	0.0
Hexan-1-ol	1.6	10.8	9.9	0.0	0.0
2-Phenylethan-1-ol	29.8	17.3	5.9	32.0	34.1
Octan-1-ol	0.1	0.2	0.6	0.1	0.0
Decan-1-ol	0.1	0.1	0.6	0.1	0.0
Dodecan-1-ol	0.1	0.1	0.6	0.1	0.0
Tetradecan-1-ol	0.1	0.2	0.6	0.1	0.0
Ethanal	9.4	6.5	58.2	9.9	0.0
Methanoic acid	32.7	4.8	5.1	37.7	37.6
Ethanoic acid	120.3	0.1	25.3	142.4	137.2
Propanoic acid	1.2	0.7	0.4	1.3	1.4
Butanoic acid	1.6	1.2	0.9	1.7	1.7
2-Methylpropanoic acid	1.7	1.2	1.1	1.7	1.7
3-Methylbutanoic acid	0.9	0.6	1.2	1.0	0.9
Hexanoic acid	3.2	6.0	2.5	2.6	3.3
Octanoic acid	4.6	23.1	24.6	1.0	0.7
Ethyl ethanoate	18.9	116.7	116.8	0.0	0.0
Ethyl butanoate	0.4	2.1	2.6	0.1	0.0
3-Methylbutyl ethanoate	0.7	4.1	4.5	0.1	0.0
Ethyl hexanoate	0.9	5.2	5.5	0.1	0.0
Hexyl ethanoate	0.1	0.1	0.6	0.1	0.0
2-Phenylethyl ethanoate	0.1	0.1	0.6	0.1	0.0
Ethyl octanoate	1.8	11.4	11.4	0.0	0.0
Diethyl butane-1,4-dioate	0.1	0.2	0.1	0.1	0.1
Ethyl decanoate	1.5	9.0	9.0	0.0	0.0
3,7-Dimethylocta-1,6-dien-3-ol	0.1	0.2	0.6	0.1	0.0

ethanoate, 2-phenylethyl ethanoate and 3,7-dimethylocta-1,6-dien-3-ol), relatively high deviations are obtained in both vinasse and distillate mass flows.

The origin of the deviations is mainly related to an important uncertainty in chemical analysis, but also to the sensitivity of concentrations to small perturbations of the steady state operation (Batista et al., 2012). In relation to the simulation module, the accuracy of concentration predictions can also be affected by the operating parameters tuned in the first level (for instance the tray efficiency) as well as by the interaction parameters of the NRTL model, most of which were fitted to experimental data with average deviations for vapor mole compositions between 1% and 27%.

Despite this important variability, a global comparison of the data set, depicted in Fig. 7, shows that simulation is rather well correlated to experimental data, with determination coef-

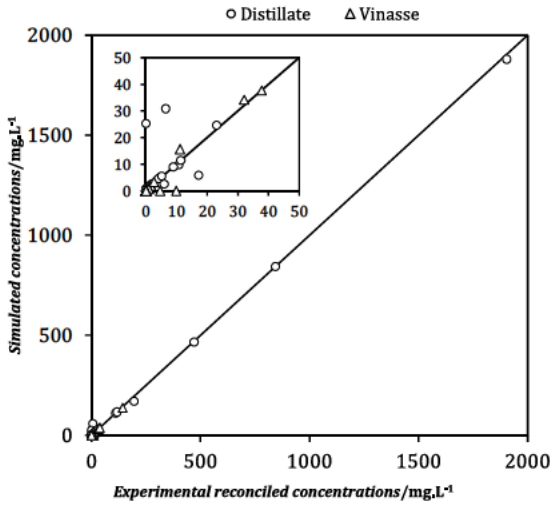

Fig. 7 – Comparison between experimental and simulation data of aroma compounds concentrations.

ficients (R^2) of 0.91 for distillate concentrations and 0.94 for vinasse concentrations. From a qualitative point of view, as indicated by (Batista et al., 2012), this result enables us to validate the ability of simulation to represent the distillation process.

For a better insight into the volatile aroma compounds behavior, a comparison of the mass recovery from feed to distillate is presented in Fig. 8. Global good agreement is obtained between experimental and simulation data. However, for a group of nine compounds already identified (butan-1-ol, octan-1-ol, decan-1-ol, dodecan-1-ol, tetradecan-1-ol, ethanal, hexyl ethanoate, 2-phenylethyl ethanoate and 3, 7-dimethylocta-1, 6-dien-3-ol), the simulation predicts an integral recovery in the distillate, whereas the experimental recovery is only between 11% and 33%. This results reveals specific issues in data acquisition: for octan-1-ol, decan-1-ol, dodecan-1-ol, tetradecan-1-ol, hexyl ethanoate, 2-phenylethyl ethanoate and 3,7-dimethylocta-1,6-dien-3-ol, the deviations can be associated with a high incertitude of the chemical analysis, due to very low concentrations, smaller than the quantification GC limit in some cases (0.1 mg L^{-1} for these species). Concerning ethanal and butan-1-ol, even if the concentrations are not very low, the deviations are also linked to the analysis technique, because their quantification GC limits are particularly high (between 5.0 and 10.0 mg L^{-1}). In the case of octan-1-ol, decan-1-ol, dodecan-1-ol, tetradecan-1-ol and hexyl ethanoate, it should be pointed out that the interaction parameters of the NRTL model were estimated from UNIFAC predictions without validation against experimental data. This could be a source of error in simulation, however, the trend displayed in Fig. 8 (distillate recovery of 100% for volatile aroma compounds of similar nature) suggests that the origin of deviations are rather associated to experimental data.

A comparison with literature data is presented in Table 8. These data were acquired from distillation of 58 wine samples in 77 different distillation units. General good agreement is verified with experimental and simulation data from this work. Recoveries higher than 100% in the literature set are due to the combined effect of analysis errors and possible chemical reactions. Indeed, an important proportion of ethyl esters from fatty acids (ethyl hexanoate, ethyl octanoate and ethyl

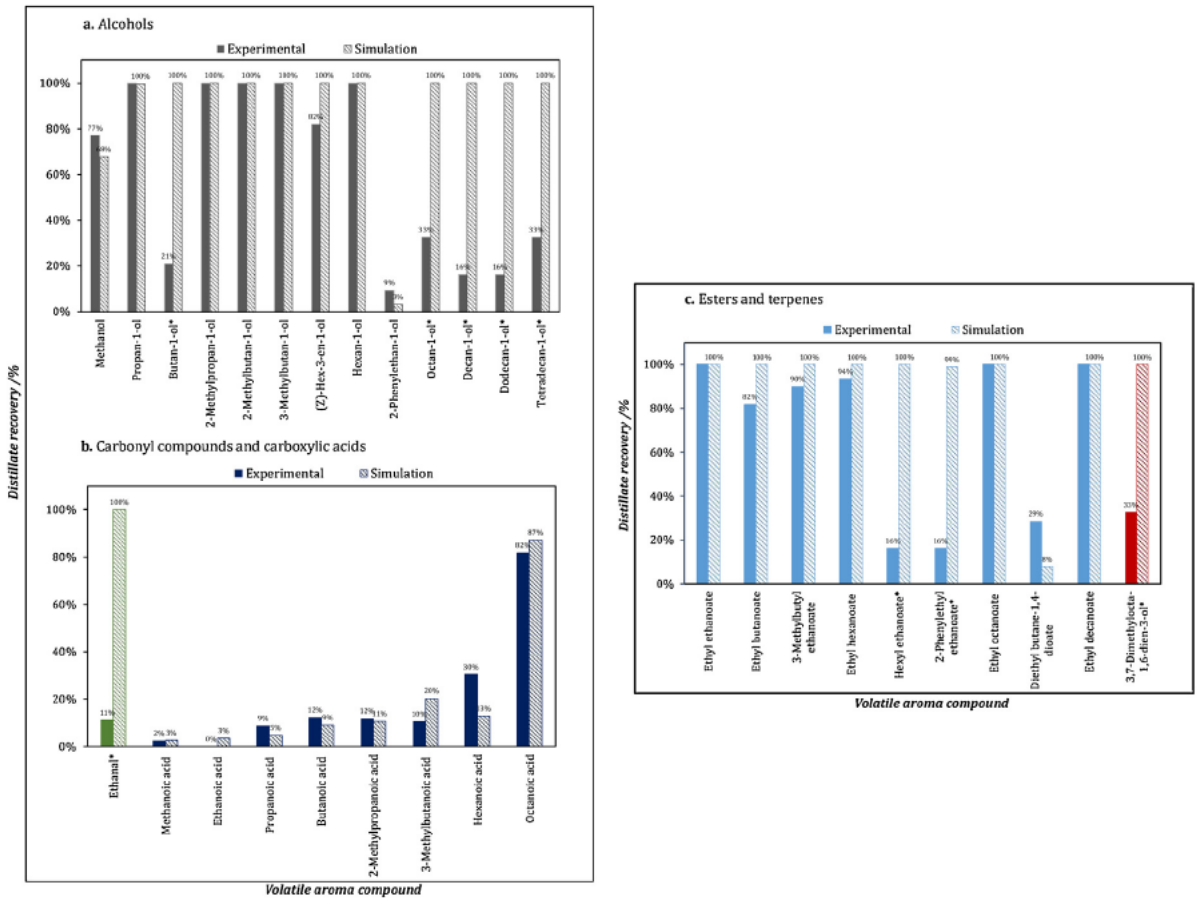

Fig. 8 – Comparison between reconciled experimental and simulation data of the aroma compounds recovery in distillate at the nominal operation point. (*) Compounds with important deviations between experimental and simulation values.

Table 8 – Comparison with literature data of the volatile aroma compounds recovery in the distillate. The literature data are average values of 80 Armagnac distillates before aging, taken from (Segur and Bertrand, 1992).

Aroma compound	Recovery in distillate /%		
	Reconciled experimental	Simulation	Literature
Methanol	77%	68%	87%
Propan-1-ol	100%	100%	98%
2-Methylpropan-1-ol	100%	100%	105%
2-Methylbutan-1-ol	100%	100%	103%
3-Methylbutan-1-ol	100%	100%	101%
2-Phenylethan-1-ol	9%	3%	10%
Ethyl ethanoate	100%	100%	94%
3-Methylbutyl ethanoate	90%	100%	90%
Ethyl hexanoate	94%	100%	104%
Hexyl ethanoate	16%	100%	100%
2-Phenylethyl ethanoate	16%	99%	84%
Ethyl octanoate	100%	100%	203%
Ethyl decanoate	100%	100%	385%
Ethanoic acid	0%	3%	5%
Hexanoic acid	30%	13%	25%
Octanoic acid	82%	87%	75%

decanoate in this case) is released by heating of yeasts present in wine during distillation (Segur and Bertrand, 1992).

In light of these results, the simulation module can be validated as a tool to represent the behavior of volatile aroma compounds in continuous Armagnac distillation, with both qualitative and quantitative precision for the estimation of distillate recoveries and good qualitative reproduction of concentrations in distillate and vinasse.

3.1.2.2. *Classification of volatile aroma compounds*. With the aim of identifying general trends on volatile aroma compounds behavior, a systematic classification is proposed. The criterion is based on phase equilibria and composition profiles. The first step was developed by the authors in a companion paper (Puentes et al., 2018a). The knowledge of vapor–liquid equilibria enables us to classify the volatile aroma compounds in three main groups, according to their relative volatilities with respect to ethanol (light key) and water (heavy key). The group I correspond to light compounds, species that are more volatile than ethanol and are therefore mainly recovered in distillate. The group II gathers the intermediary compounds, which are distributed between distillate and vinasse due to their intermediate volatilities. The group III correspond to heavy compounds, less volatile than ethanol and water, thus mainly recovered in the vinasse.

This classification depends on the liquid composition interval. In Table 9, two classifications are proposed: one over the whole ethanol mole range ($0 < x_{Et} < 1$), proposed in the original paper, and another over the ethanol mol range of the liquid phase simulated in the distillation column of this work ($0 < x_{Et} < 0.1$). In the current case, 20 species are classified as light compounds, 10 as intermediary compounds and 2 as heavy compounds. Among light compounds, more than a half were classed as intermediary compounds when considering the whole concentration range, but their behavior changes because the relative volatilities with respect to ethanol are higher in the region of low ethanol concentration.

Now, using the simulation results, it is possible to identify different trends for the composition profiles inside the column. These trends are depicted in Fig. 9, where the mole fractions of volatile aroma compounds in the vapor and liquid phases are presented at the different stages of the column, from the partial condenser (stage 1) to the boiler (stage 14). In the case of light compounds (Fig. 9a) and heavy compounds (Fig. 9e) the composition profiles are monotonous. A light compound is concentrated in the vapor phase while stripped from the liquid one. A heavy compound exhibits a behavior completely opposed, being concentrated in the liquid phase. On the other hand, a detailed analysis of the composition profiles for intermediary compounds evidences the existence of 3 different profiles: in the first profile, presented in Fig. 9b, there is a net concentration of the vapor and stripping of the liquid, but in comparison to the profile of light compounds, the ratio of vapor-liquid mole fraction is lower in every stage. In the second and third profiles, depicted in Figs. 9c and 9d, the aroma compound is stripped from the vapor phase, to such an extent that the distillate mass fraction becomes smaller than the vinasse one. The crossing of vapor and liquid profiles indicates that there is an inversion of the molar composition ratio, from $y/x > 1$ to $y/x < 1$. The differences between those two profiles are related to the profile shape and to the recovery levels of the aroma compound in the distillate.

In this way, a more precise classification of the intermediary compounds can be proposed by considering this difference of composition profiles. The resulting classification is comprised of the three groups proposed in the previous classification (I for light compounds, II for intermediary compounds and III for heavy compounds), with three new subgroups for intermediary compounds: II.1, II.2 and II.3. The description of each group is completed with some factors that characterize the separation, including: ratio of vapor-liquid mole fractions in every tray, recovery in distillate, profile shape, and variation of composition in both phases throughout the column. A final synthesis of this classification is presented in Table 10.

3.2. *Validation of the simulation of heads and tails extraction*

The circuits of heads and tails extractions are used in spirits production to modify the distillate composition. As described in Section 2.1 and shown in Fig. 2, both circuits are placed in the coil of the distillate flow inside the wine heater. The tails circuit allows the extraction of a fraction of liquid formed at the beginning of the vapor condensation. The extraction is done from the bottom of the first turn of the coil. In the heads

Table 9 – Classification of volatile aroma compounds according to their relative volatility with respect to ethanol and water in two liquid composition intervals defined by the ethanol mole fraction, xEt.

$0.0 < x_{Et} < 1.0$ (Puentes et al., 2018a)		$0.0 < x_{Et} < 0.1$ (This work)	
Group	Compound	Group	Compound
I. Light	Octan-1-ol	I. Light	Octan-1-ol
	Decan-1-ol		Decan-1-ol
	Dodecan-1-ol		Dodecan-1-ol
	Tetradecan-1-ol		Tetradecan-1-ol
	Ethanal		Ethanal
	Ethyl ethanoate		Ethyl ethanoate
	Ethyl butanoate		Ethyl butanoate
	Hexyl ethanoate		Hexyl ethanoate
	Propan-1-ol		Propan-1-ol
	Butan-1-ol		Butan-1-ol
	2-Methylpropan-1-ol		2-Methylpropan-1-ol
	2-Methylbutan-1-ol		2-Methylbutan-1-ol
	3-Methylbutan-1-ol		3-Methylbutan-1-ol
	(Z)-Hex-3-en-1-ol		(Z)-Hex-3-en-1-ol
	Hexan-1-ol		Hexan-1-ol
II. Intermediary	3-Methylbutyl ethanoate	II. Intermediary	3-Methylbutyl ethanoate
	Ethyl hexanoate		Ethyl hexanoate
	Ethyl octanoate		Ethyl octanoate
	Ethyl decanoate		Ethyl decanoate
	3,7-Dimethylocta-1,6-dien-3-ol		3,7-Dimethylocta-1,6-dien-3-ol
	Methanol		Methanol
	2-Phenylethan-1-ol		2-Phenylethan-1-ol
	Propanoic acid		Propanoic acid
	Butanoic acid		Butanoic acid
	2-Methylpropanoic acid		2-Methylpropanoic acid
	3-Methylbutanoic acid		3-Methylbutanoic acid
	Hexanoic acid		Hexanoic acid
	Octanoic acid		Octanoic acid
	2-Phenylethyl ethanoate		2-Phenylethyl ethanoate
	Diethyl butane-1,4-dioate		Diethyl butane-1,4-dioate
III. Heavy	Methanoic acid	III. Heavy	Methanoic acid
	Ethanoic acid		Ethanoic acid

Table 10 – Classification of the volatile aroma compounds according to the composition profile in the distillation column.

Group	Profile type	Volatile aroma compound		Ratio y_{AC}/x_{AC}		Distillate recovery (%)		Profile shape	Variation of concentration	
				Min	Max	Min	Max		Vapor phase	Liquid phase
Light	I	20	(Table 9)	0.07	>16	100%	100%	Monotonous	Concentration	Stripping
Intermediary	II.1	4	Methanol; 3-methylbutanoic acid, octanoic acid; 2-phenylethyl ethanoate	1.5	18	68%	99%	Concavity change	Concentration	Stripping
	II.2	4	Butanoic acid, 2-methylpropanoic acid, hexanoic acid; diethyl butane-1,4-dioate	0.5	7.6	8%	20%	Concavity change	Stripping	Stripping
	II.3	2	2-Phenylethan-1-ol; propanoic acid	0.3	1.2	3%	5%	Monotonous	Stripping	No variation
Heavy	III	2	Methanoic acid, ethanoic acid	0.4	0.8	3%	3%	Monotonous	Stripping	Concentration

circuit, a fraction of the remaining vapor is withdrawn over the last turn of the coil, before the cooling section. Both circuits are sent to the external compartment of the wine heater, in order to cool the extractions before evacuation from the device.

The simulation module was tested to reproduce the operation of both circuits, using a vapor-liquid flash for their modeling. Two specifications were considered to solve the problem: the ABV of the extraction, used to fix the refrigeration power required to condense a fraction of the vapor distillate, and the mass flow, used to verify the proportion distillate–extraction. The configuration of these theoretical circuits is presented Fig. 10. Since the extractions are placed in the wine heater, mass and energy balances of the column are invariable with respect to the nominal operation point.

The data required for this simulation were acquired during the experimental campaign, just after characterization of the nominal operation point. Two independent experiments, one for each extraction, were carried out: the extraction valve was completely opened during 15 min. 5 min after opening, extraction and new distillate mass flows were measured using the

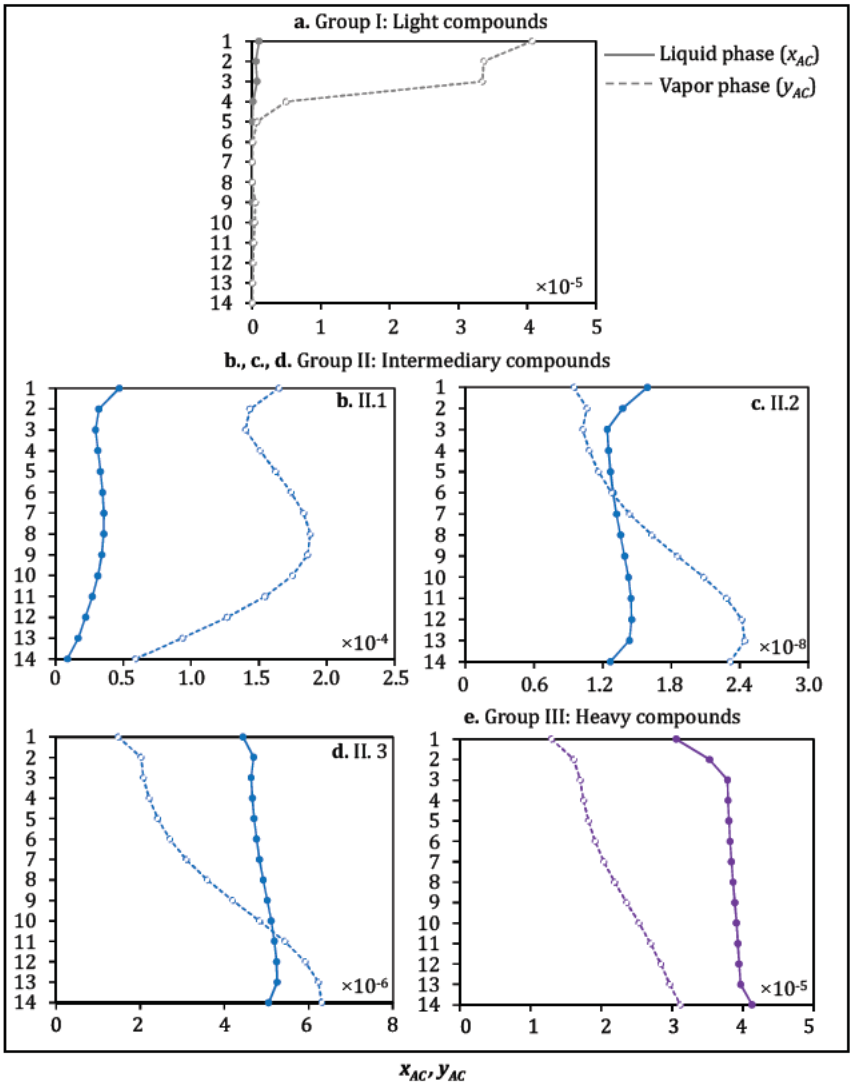

Fig. 9 – Main types of composition profiles of aroma compounds through the distillation column. Specific profiles for: (a) ethyl ethanoate, (b) methanol, (c) diethyl butane-1,4-dioate, (d) 2-phenylethan-1-ol and (e) ethanoic acid.

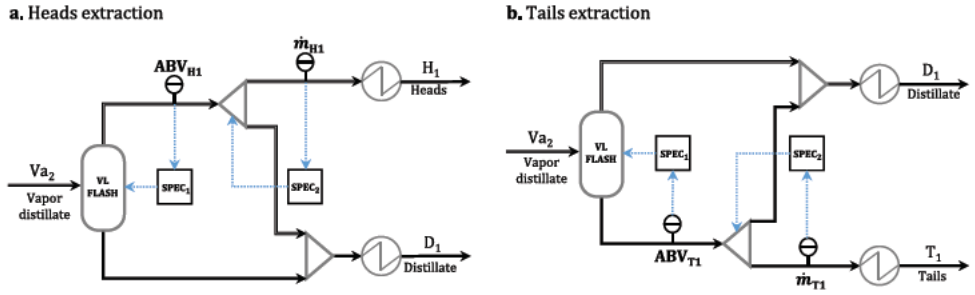

Fig. 10 – Configuration for the simulation of (a) heads and (b) tails extractions. SPEC$_1$ and SPEC$_2$ are control loops to verify the respective experimental values of ethanol composition (ABV) and mass flow ($\dot{m}$) of the extraction.

same technique described in Section 2.2.1. Each measurement was made in duplicate. Relative uncertainty for distillate was lower than 0.1% and about 2.3% for heads and tails extractions. At the end of this period, liquid temperatures were measured, using the Pt100 probe for the extraction and the mercury thermometer for the distillate after extraction. The ABV was also quantified with the DMA35 density meter. Finally, a single 700 mL sample of each stream was taken for chemical analysis, following the methodology already described. After reconciliation, the ABV and mass flow were respectively 80.1%v/v and 14.7 kg h^{-1} for heads extractions and respectively 40.3%v/v and 19.4 kg h^{-1} for tails extractions.

To analyze the performance of both circuits, an extraction coefficient is defined with respect to ethanol:

$$\varepsilon_{AC/Et,e} = \frac{x_{mAC,e}/x_{mEt,e}}{y_{mAC,Va2}/y_{mEt,Va2}} \quad (11)$$

where $\varepsilon_{AC,e}$ is the extraction coefficient of a volatile aroma compound in the circuit e (heads H_1 or tails T_1), $x_{mAC,e}$ and $x_{mEt,e}$ are the respective mass fractions of volatile aroma compound and ethanol in the extraction e, and $y_{mAC,Va2}$ and $y_{mEt,Va2}$ are the respective mass fractions in the stream Va_2, which corresponds to the vapor distillate before extraction.

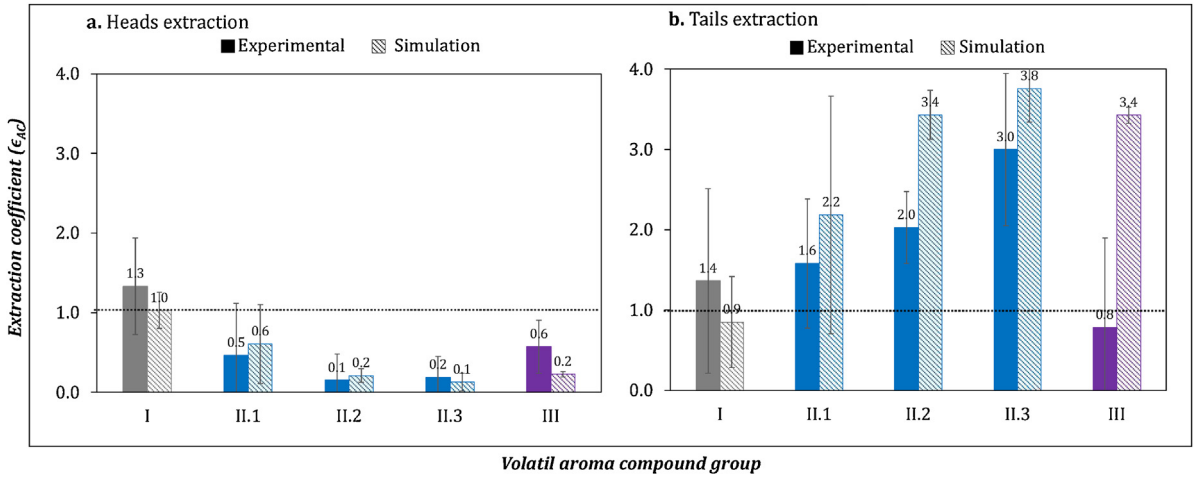

Fig. 11 – Extraction coefficients of the volatile aroma compounds in (a) heads circuit and (b) tails circuit. Average experimental and simulation values for the different groups of volatile aroma compounds: light (I), intermediary (II) and heavy (III). In this simulation, the mass and energy balances of the column remains invariable with respect to the nominal operation point.

A value of $\varepsilon_{AC/Et,e}$ higher than 1 indicates that the extraction of the aroma compound is favorable with respect to ethanol.

For the three groups of volatile aroma compounds proposed in the previous section, average values of $\varepsilon_{AC,e}$ with their respective uncertainties are presented in Fig. 11. Only the volatile aroma compounds whose behavior was correctly validated against experimental data are considered in this analysis. From the initial group of 32 species, nine were not included (butan-1-ol, octan-1-ol, decan-1-ol, dodecan-1-ol, tetradecan-1-ol, ethanal, hexyl ethanoate, 2-phenylethanoate and 3,7-dimethylocta-1,6-dien-3-ol). A reliable comparison would not be possible because the concentration of these compounds were too low in one of the process flows.

Concerning heads extraction, the extraction coefficients follow a decreasing trend from the light compounds (group I) to heavy compounds (group III). This trend is verified with both experimental and simulation data, except for the group III, for which the average experimental extraction coefficients are 0.6, against 0.2 from simulation. The inversed trend is identified for tails extraction. The deviations between experimental and simulation data may be attributed to sensitivity and accuracy issues of the analysis technique. Moreover, since the calculation of the extraction coefficients depends on two streams, extraction and distillate, the uncertainty of this variable can be amplified.

In relation to the role of each circuit, the trends identified by the profiles are logic in principle. While a heads circuit is due to extract very volatile species, in a tails circuit low volatile species that condense quickly should be evacuated. Nonetheless, in the heads circuit here simulated, the extraction coefficients for light compounds are close to 1 (group I, average between 1.3 and 1.0), which means that the distillate composition is modified but not in the desired way. A preferential passage of lights compounds with respect to ethanol, reflected in higher extraction coefficients, was expected. The results are more favorable for the tails circuit, particularly regarding simulation data, because the average extraction coefficients for intermediary (group II) and heavy compounds (group III) are considerably higher than 1, between 2.5 and 3.4. In this case, the extraction leads to a real modification of the distillate composition with elimination of the targeted species.

For the group of compounds simulated, one can conclude that only the tails circuit works correctly. The heads circuit is probably not well placed, and a different distribution would be required to favors the preferential extraction of light compounds with respect to ethanol. Nonetheless, it is important to point out that the volatility of the species included in the simulation is not much higher than that of ethanol at the involved liquid composition interval. More volatile species (such as 1,1-diethoxyethane, ethanal, propanal and butanal, according to Puentes et al., 2018a) should thus be taken into account to evaluate the real impact of this circuit.

3.3. *Analysis by simulation of the influence of operating parameters*

After validation of the simulation in the nominal operation point, a parametric analysis was performed to study the influence of operating parameters on ethanol and volatile aroma compounds behavior. Again, only volatile aroma compounds whose representation was satisfactory regarding experimental data are considered.

3.3.1. *Ethanol concentration in the distillate*

Several authors have suggested an important influence of the distillate alcoholic strength on the separation of volatile aroma compounds. The simulation module was used to vary the ABV of distillate between 59%v/v and 72%v/v, by modifying the reflux ratio through the condensation power, (Fig. 12a). It was not possible to simulate the lowest permitted ABV (52%v/v), given the initial wine ABV and the presence of a top partial condenser. For comparison purposes, the ethanol mass flow in the distillate was fixed to the nominal value in all the simulations (72.65 kg h^{-1}). Therefore, to verify ethanol mass balance in the column, the net heating power in the boiler was tuned using a specification. As expected, according to Fig. 12b, the evolution of distillated ABV and mass flow with reflux ratio are inverse. The minimum ABV possible in this installation, obtained when the condensation is only generated by thermal losses (=0.4 kW), is around 59%v/v. With respect to the nominal operation point, the condensation power must be doubled (from 11.6 kW to 23.4 kW) to increase the ethanol strength to 72%v/v. The net heating power is also increased but the variation is considerably lower, of 2.5% (from 88.5 kW to 90.8 kW).

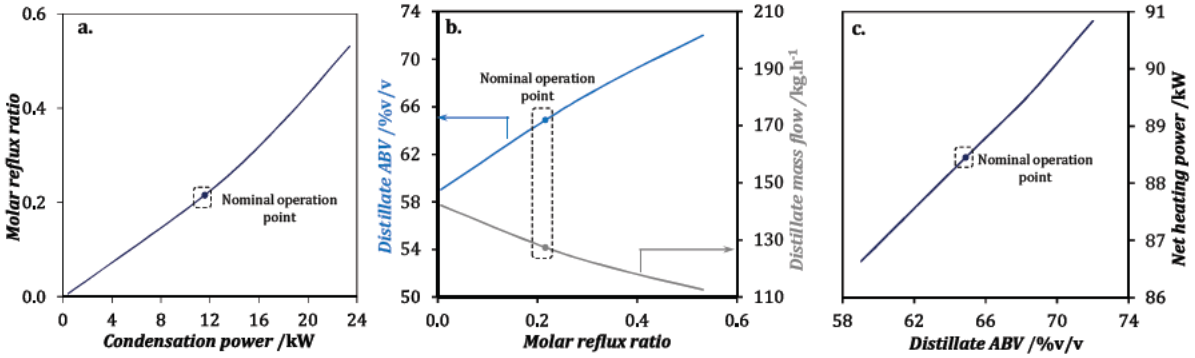

Fig. 12 – (a) Variation of reflux ratio with condensation power. (b) Influence of reflux ratio on distillate ethanol concentration and mass flow. (c) Influence of ethanol concentration on heat power. In these simulation the ethanol mass flow in the distillate was fixed to the nominal point value.

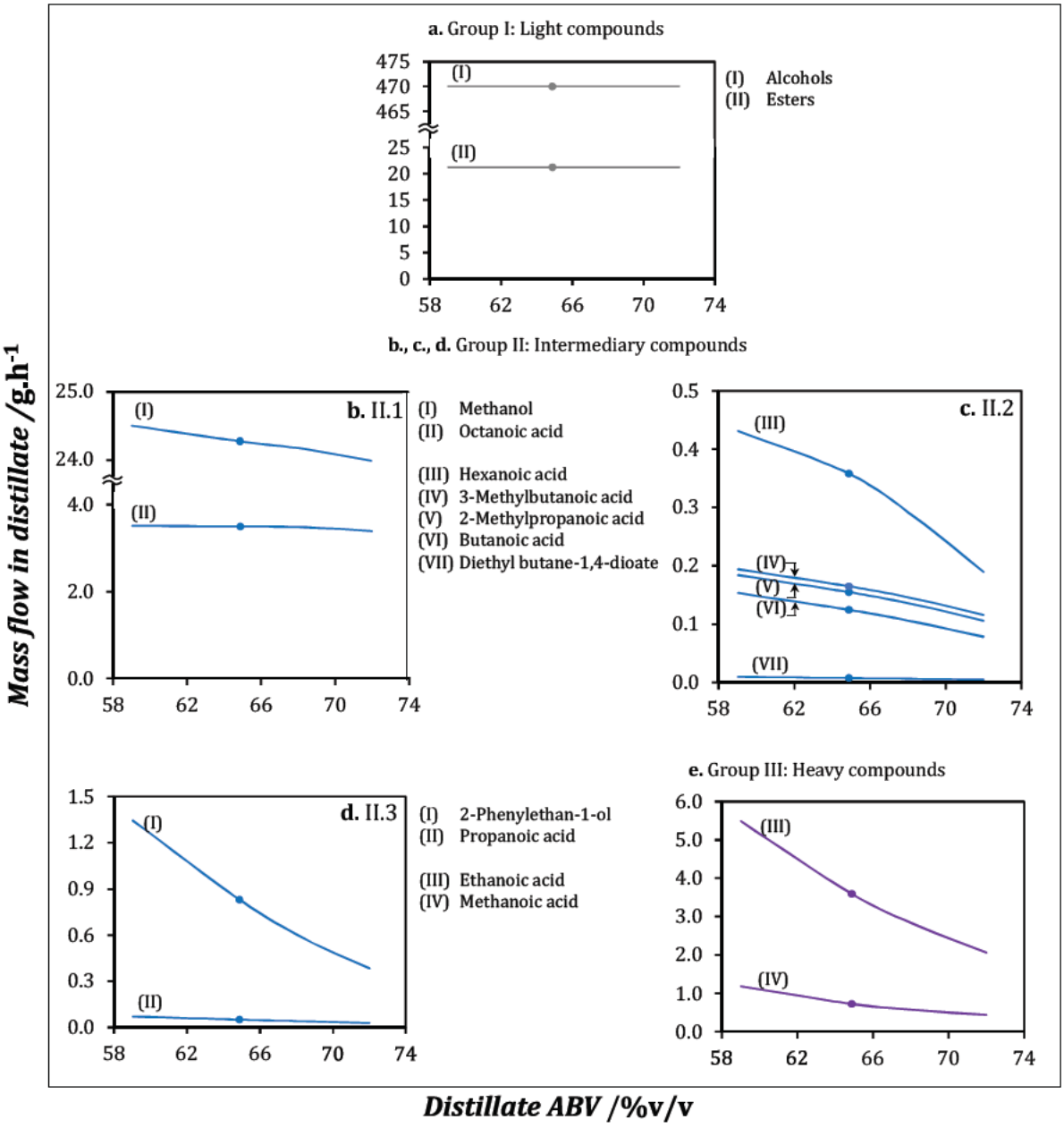

Fig. 13 – Influence of ethanol concentration in the distillate on volatile aroma compounds partial mass flows. In this simulation, the ethanol composition in distillate was modified with the reflux ratio, which was in turn modified with the condensation power. The ethanol mass flow in the distillate was fixed to the nominal point value.

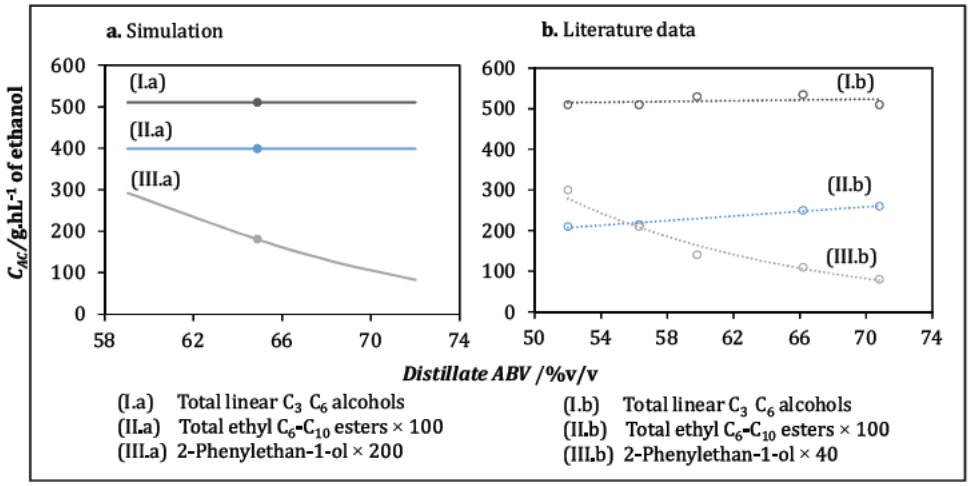

Fig. 14 – Comparison with literature data of the volatile aroma compounds concentration in the distillate as a function of the ethanol concentration. Literature data taken from (Segur and Bertrand, 1992).

In the case of volatile aroma compounds, the evolution of distillate partial mass flows with ABV are presented in Fig. 13. Species from the group I (light compounds) are not affected by changes on the alcohol strength, a logic result because they are more volatile than ethanol and are integrally recovered in the distillate. For the other groups, the partial mass flow decreases when the ABV is increased. The variation is slight for intermediary compounds of the subgroup II.1, but the effect is pronounced for the subgroups II.2, and II.3 as well as for heavy compounds, group III. The concentrations of volatile aroma compounds with respect to ethanol in the distillate follow the same evolution, as the ethanol mass flow in the distillate does not change. This behavior has already been discussed in the literature and demonstrates that the modification of operating parameters (condensation power in this case) do have an impact on the distillate composition. High concentrations of some intermediary and heavy compounds are favorable for aging purposes, due to their 'winey' character, but for young commercial spirits, without aging, their limitation in the distillate, and therefore operation at high reflux ratio, is recommended (Segur and Bertrand, 1992; Bertrand et al., 1998; Decloux and Joulia, 2009).

A comparison between simulation and literature data is given in Fig. 14, where the concentration in absolute ethanol is presented as a function of distillate ABV. The trends obtained are the same: no variation for linear C_3–C_6 alcohols (from propan-1-ol to hexan-1-ol) as well as ethyl C_6–C_{10} esters (from ethyl hexanoate to ethyl decanoate) and significant reduction for 2-phenylethan-1-ol. The literature data for ethyl esters are slightly rising, but according to the authors, this is a bias provoked by experimental mass losses of ethanol at high ABV. For this latter group and 2-phenylethan-1-ol, the original concentrations (without the multiplication factors used exclusively for representation purposes) are different from the simulated values, but this can be explained simply by differences in wine composition. Indeed, wine intended for Armagnac production can come from 10 different grape varieties and its TAV is between 7.5% and 12%v/v (JORF, 2015), which can reflect non negligible variations in the aroma compounds composition. Despite those slight differences, this comparison validates simulation and demonstrates its utility in the analysis of operating parameters, with the benefit of both cost and time saving.

3.3.2. *Thermal losses*

Thermal losses through the column walls represent between 40% and 50% of total thermal losses in Armagnac distillation units (Marty and Cluzeau, 2010). To analyze this parameter, three simulation scenarios were considered: the nominal operation as reference point (thermal losses of 2.8 kW), a point with minimal thermal losses, fixed at 0.4 kW (the contribution of thermal losses to condensation power) and a point with doubled losses, 5.6 kW. For these simulations, the ethanol losses in vinasse as well as the condensation power were fixed at the nominal values. The results displayed in Fig. 15, show that the reduction of thermal losses has an antagonist impact, since both net heating power and distillate ABV decrease. The reduction of alcoholic strength confirms the reflux effect of thermal losses on the column. However, the variation is small with respect to the nominal point, 0.5% regarding ABV and 2.3% in the case of heating power.

Impact on distillate composition was also studied, but no significant variation of concentrations was detected for any of the aroma compounds groups. This result can be explained by the little variation of the distillate ABV and suggests, at least for the compounds here simulated, that the isolation of the distillation unit would not modify the spirit composition. In these conditions, isolation would be an advantaging solution to reduce energy consumption (about 2 kW) while maintaining both ethanol recovery and spirit composition. However, experimental validation would be still necessary to verify the real impact on product quality.

3.3.3. *Distillate temperature after condensation*

To conclude the analysis, a theoretical effect of the distillate temperature on the spirits composition was analyzed by means of the Simulis Thermodynamics® calculator. This parameter has a practical interest because the condensed distillate is directly exposed to the atmosphere during its evacuation, before storage. Using the NRTL model and the corresponding interaction parameters, the partial pressure of all the species were calculated at four temperatures, T = 12 °C, T = 15 °C, T = 25 °C and T = 28 °C. The composition of the liquid phase was fixed at the reconciled experimental set reported in this work. By defining the reference temperature as the lowest value (T = 12 °C), the variations of partial pressure of the volatile aroma compounds due to temperature increases

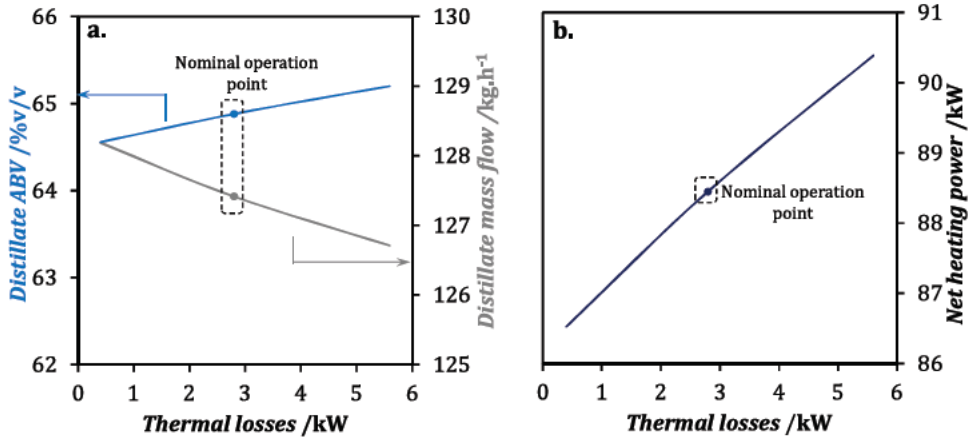

Fig. 15 – Influence of heat losses on (a) distillate ethanol composition and mass flow and, (b) heat power. In this simulation, the ethanol losses in the bottoms as well as the condensation power were fixed at the nominal point values.

(25%, 108% and 133%) were calculated and compared to those of ethanol, equivalent to 21%, 119% and 159%.

The results are presented in Table 11. Two types of behavior can be identified, independent of the compounds classification: (i) increases of partial pressure with the same order of magnitude of ethanol increase (between 0.8 and 1.4 times in the case of methanol, propan-1-ol, 2-methylpropan-1-ol, methanoic acid, ethanoic acid, propanoic acid, ethyl ethanoate, ethyl butanoate, 3-methylbutyl ethanoate, ethyl hexanoate), and (ii) increases of partial pressure considerably higher than that of ethanol, between 1.4 and 2.8 times (case of 2-methylbutan-1-ol, 3-methylbutan-1-ol, (Z)-hex-3-en-1-ol, hexan-1-ol, 2-phenylethan-1-ol, 2-methylpropanoic acid, butanoic acid, 3-methylbutanoic acid, hexanoic acid, octanoic acid, ethyl octanoate, ethyl decanoate, diethyl butane-1,4-dioate). The second behavior, associated with non-linear (2-phenylethan-1-ol for instance) or high molar mass molecules, suggests that it is possible to entail a preferential evacuation of these molecules to the atmosphere, whose effect is all the more relevant when the distillate temperature is higher.

This result should not be overestimated as it is derived only from theoretical calculations. In general, to define the real impact of distillate temperature and other operating parameters on product quality, it would be necessary to integrate simulation with sensory and olfactometric analysis, which would allow a better understanding of the specific role of each compound, and its concentration, on the organoleptic properties of spirits.

4. Conclusions

In this work, a module for the simulation of spirits distillation at steady state was developed and validated using the commercial software ProSimPlus®. A thorough analysis of an Armagnac production unit was performed, considering a model solution composed by ethanol, water and 32 volatile aroma compounds that may have an impact on product quality.

Comparison with experimental data confirmed that the simulation is able to reproduce the right orders of magnitude of the volatile aroma compound concentrations and to predict with good precision the recovery from wine to distillate. High deviations for this latter parameter were identified in a group of nine compounds, which is attributed to errors in chemical analysis that conducted to incoherent mass flows, even after data reconciliation. The technique employed, gas chromatography, is very sensitive and has a limited accuracy due to the system complexity and the great variety of factors involved, including sample preparation and instrumentation. More powerful methods should be used to get better estimations. However, the gain in accuracy may imply an important increase of technical complexity, which is not strictly desirable for a simulation approach, aimed for better yet faster process design.

The knowledge of relative volatilities as well as the representation of concentration profiles inside the column made it possible to propose a classification of the volatile aroma compounds in three main groups, in particular an intermediary group for which the distribution between the distillate and the vinasse can be modified by the choice of operating conditions.

Simulation of the extraction circuits proved that only the tails circuit of the studied Armagnac unit favors a real elimination of intermediary and heavy species with respect to ethanol. Through the heads circuit it is possible to evacuate light compounds. However, for the group of compounds simulated, the extraction is not efficacious, as the average extraction coefficient for the group of light compounds is close to 1. More volatile species should be considered in the simulation to evaluate the real impact of the circuit. Otherwise, a new location in the wine heater could also be useful to promote a different distribution of light compounds between the coexisting vapor and liquid phases.

The analysis of operating parameters proved that the distillation process can modify the distillate composition. Two parameters were identified to have a real impact: ethanol concentration and distillate temperature after condensation. The increase of alcoholic strength, by modification of the condensation power, leads to a reduction of the concentration of intermediary and heavy compounds in the distillate. Concerning the temperature after condensation, the composition modification is based on a preferential elimination of non-linear and high mass molar species towards the environment. On the other hand, thermal losses have a slight effect on distillate ethanol concentration. However, at the concentration levels here evaluated, the effect on volatile aroma compounds can be neglected.

These results demonstrate that simulation is a powerful tool to better understand and predict the behavior of volatile aroma compounds in spirits distillation. The real aim is not to reproduce with high accuracy the experimental data

Table 11 – Theoretical variation of the partial pressure of aroma compounds with the cooling temperature of distillate.

Group	Compound	Mass fractions in liquid distillate	Partial pressure at $T_0 = 12\,^{\circ}C$/kPa	Increase of partial pressure/%		
				$T_f = 15\,^{\circ}C$ $\Delta T = 3\,^{\circ}C$ (25%)	$T_f = 25\,^{\circ}C$ $\Delta T = 13\,^{\circ}C$ (108%)	$T_f = 28\,^{\circ}C$ $\Delta T = 16\,^{\circ}C$ (133%)
I	Ethanol	0.57	3.32	21%	119%	159%
	Water	0.43	0.74	22%	127%	171%
	Ethyl ethanoate	1.3×10^{-4}	4.43×10^{-3}	18%	99%	130%
	Ethyl butanoate	2.4×10^{-6}	6.50×10^{-5}	18%	97%	128%
	Propan-1-ol	1.2×10^{-4}	3.51×10^{-4}	23%	139%	189%
	2-Methylpropan-1-ol	9.4×10^{-4}	1.92×10^{-3}	26%	163%	223%
	2-Methylbutan-1-ol	5.2×10^{-4}	1.48×10^{-4}	33%	231%	329%
	3-Methylbutan-1-ol	2.1×10^{-3}	9.71×10^{-4}	32%	216%	303%
	(Z)-Hex-3-en-1-ol	2.2×10^{-6}	6.26×10^{-7}	29%	191%	266%
	Hexan-1-ol	1.1×10^{-5}	1.93×10^{-6}	36%	253%	362%
	3-Methylbutyl ethanoate	4.5×10^{-6}	3.39×10^{-5}	22%	128%	172%
	Ethyl hexanoate	5.8×10^{-6}	4.71×10^{-5}	23%	137%	185%
	Ethyl octanoate	1.3×10^{-5}	7.56×10^{-6}	31%	207%	290%
	Ethyl decanoate	1.0×10^{-5}	5.65×10^{-7}	40%	298%	434%
II.1	Methanol	2.2×10^{-4}	1.84×10^{-3}	19%	103%	137%
	3-Methylbutanoic acid	6.7×10^{-7}	5.19×10^{-8}	31%	205%	287%
	Octanoic acid	2.6×10^{-5}	5.50×10^{-7}	39%	299%	438%
II.2	2-Methylpropanoic acid	1.3×10^{-6}	2.84×10^{-7}	30%	198%	276%
	Butanoic acid	1.3×10^{-6}	1.76×10^{-7}	29%	185%	257%
	Hexanoic acid	6.7×10^{-6}	5.55×10^{-8}	39%	294%	430%
II.3	Diethyl butane-1,4-dioate	2.2×10^{-7}	7.64×10^{-9}	39%	287%	416%
	2-Phenylethan-1-ol	1.9×10^{-5}	6.71×10^{-8}	39%	295%	430%
III	Propanoic acid	7.2×10^{-7}	2.51×10^{-7}	26%	165%	227%
	Methanoic acid	5.3×10^{-6}	1.15×10^{-5}	19%	106%	141%
	Ethanoic acid	1.1×10^{-7}	1.31×10^{-7}	22%	126%	170%

(whose uncertainties may be important) but to represent correctly the distillation trends and, in this way, analyze the impact of operating parameters on spirit composition and process performance. Further results of our ongoing research on Armagnac and Calvados distillation will be reported in a future work.

However, it is important to conclude that the concrete improvement of product quality goes beyond process engineering, and requires the coupling of simulation with complementary scientific tools such as reaction chemistry, sensory and olfactometric analysis.

Funding

This work was supported by the ABIES Doctoral School (AgroParisTech, Université Paris-Saclay; Doctoral contract 2014-7) and was implemented within the framework of the RMT FIDELE (Réseau Mixte Technologique Produits fermentés et distillés), with funding from the French Association ACTIA (Association de coordination technique pour l'industrie agroalimentaire).

Conflicts of interest

None.

Acknowledgments

The authors are grateful to Marie-Claude Segur, for advisory and support during the experimental campaign in Armagnac, and to the UNGDA staff, particularly Stephane Couturier, for the technical support during the samples analysis. They also wish to thank Silvère Massebeuf from ProSim, for his assistance with ProSimPlus® and Bruno Perret from INRA, for advisory in instrumentation.

APPENDIX A. Methods and validation of aroma compounds analysis

A.1 Analysis methods

Details about the analysis methods used in this work, including internal standards, pretreatment procedure and chromatographic conditions, are gathered in Table A1.

A.2 Calculation of volume concentrations

For quantification and reconciliation purposes, two parameters are required: the quantification limit and the response factor. The quantification limit of a volatile aroma compound (QL_{AC}) is the minimal concentration that can be estimated with an acceptable level of accuracy and repeatability at specific separation and detection conditions. This limit can be determined graphically as a function of the background noise in a chromatogram. For its part, the response factor of a volatile aroma compound is defined as the ratio between its concentration and the associated chromatographic peak area. In order to minimize the variability introduced by peak areas, this ratio is compared to the corresponding ratio of an internal standard. The response factor is obtained from the analysis of a calibration solution of known composition. The formula is:

$$RF_{AC/IS} = \frac{A_{IS^\circ} C_{AC^\circ}}{A_{AC^\circ} C_{IS^\circ}} \quad \text{(A1)}$$

here, $RF_{AC/IS}$ is the response factor (dimensionless) of a volatile aroma compound AC with respect to an internal standard IS, C_{AC° is the concentration (in $mg\,L^{-1}$) of the volatile aroma

Table A1 – Analysis methods implemented in this work for the quantification of volatile aroma compounds after ABV adjustment. e: column thickness, V: volume of injection, D_O: initial volume flow, D_F: final volume flow, T_O: initial temperature, T_F: final temperature, t: time, R_i: increase i of volume flow or temperature.

Method	Description	Instrumentation
Direct injection-GC/FID	*Chemical families analyzed* Acetals, alcohols, carbonyl compounds, esters, furans *Internal standard* 4-Methylpentan-2-ol	*Chromatograph:* HP 6890 *Column:* Type: Polar capillary CP WAX 57 CB (Agilent CP97753) Dimensions: 50 m × 0.32 mm, e=0.25 μm *Mobile phase:* Gas: Hydrogen, $D_O = 2.0\,mL\,min^{-1}$ – t = 21.5 *min* $R_1 = 1.0\,mL\,min^{-2}$, $D_F = 2.5\,mL\,min^{-1}$ – t = 13.50 min *Injection:* Split: 1/30. V = 1 μL *Oven:* $T_O = 35\,°C$ – t = 10 min R_1=5 °C min^{-1}, $T_F = 100\,°C$ – t = 0 min R_2=15 °C min^{-1}, $T_F = 200\,°C$ – t = 5 min *Detector:* T = 220 °C
Liquid–liquid extraction- GC/FID	*Chemical families analyzed* Acetals, alcohols, esters, furans, terpenes *Internal standard* Ethyl tridecanoate, Methyl heptanoate, Methyl heneicosanote *Pre-treatment* *Low ABV:* Extraction using a mixture of 2,2,4-trimethylpentane/ethoxyethane (75%/25%v/v) with sodium chloride in saturated aqueous sodium carbonate solution ($250\,g\,L^{-1}$). *High ABV:* Extraction using 2,2,4-trimethylpentane with sodium bicarbonate/sodium chloride (5%/95% mass).	*Chromatograph:* HP 7890B *Column:* Type: Polar capillary DB WAX (Agilent 122-7062) Dimensions: 60 m × 0.25 mm, e = 0.25 μm *Mobile phase:* Gas: Hydrogen, $D_O = 2.1\,mL\,min^{-1}$ *Injection:* Split: 1/30, V=2 μL *Oven:* $T_O = 35\,°C$ – t=0 min R_1=20 °C.min^{-1}, $T_F = 60\,°C$ – t = 0 min R_2=3 °C.min^{-1}, $T_F = 120\,°C$ – t = 0 min R_2=4 °C min^{-1}, $T_F = 220\,°C$ – t = 18 min *Detector:* T = 220 °C
Derivatization-GC/FID	*Chemical families analyzed* Carboxylic acids *Internal standard* (2E)-But-2-enoic acid *Pre-treatment* *Low ABV:* Isolation of acids by steam distillation at constant volume. Neutralization with tetrabutylammonium hydroxide. Drying with nitrogen and then in an oven for 30 min at 45 °C. Derivatization with benzyl bromide for 1 h in an oven *High ABV:* Neutralization of acids with tetrabutylammonium hydroxide. Drying with nitrogen and then in an oven for 30 min at 45 °C. Derivatization with benzyl bromide for 1 h in an oven	*Chromatograph:* HP 7890B *Column:* Type: Polar capillary DB WAX (Agilent 122-7062) Dimensions: 60 m × 0.25 mm, e = 0.25 μm *Mobile phase:* Gas: Hydrogen, D_O=2.1 mL min^{-1} *Injection:* Split: 1/30, V = 2 μL *Oven:* $T_O = 35\,°C$ – t = 0 min R_1=20 °C min^{-1}, $T_F = 60\,°C$ – t = 0 min R_2 = 3 °C min^{-1}, $T_F = 120\,°C$ – t = 0 min R_2 = 4 °C.min^{-1}, $T_F = 220\,°C$ – t = 18 min *Detector:* T = 220 °C

compound AC in the calibration solution, C_{IS° is the concentration (in $mg\,L^{-1}$) of the internal standard in the same solution, A_{AC° is the peak area (dimensionless) associated to the volatile aroma compound and A_{IS° is the peak area (dimensionless) for the internal standard.

The estimated values of quantification limits in $mg\,L^{-1}$ and response factors in both low and high ABV samples are presented in Table A2 for each aroma compound.

The concentrations of volatile aroma compounds in the process samples were estimated using the response factors and the chromatographic data. The equation is:

$$C_{AC,j} = \frac{RF_{AC/IS} k_C A_{AC,j} C_{IS,j}}{A_{IS,j}} \quad (A2)$$

where $C_{AC,j}$ is the concentration (in $mg\,L^{-1}$) of a volatile aroma compound AC in a sample of the process stream j, $RF_{AC/IS}$ is the corresponding response factor (dimensionless) determined at the same analysis conditions, $A_{IS,j}$ and $A_{AC,j}$ are the peak areas (dimensionless) of internal standard and volatile aroma compound AC in the analyzed sample, $C_{IS,j}$ is the concentration (in $mg\,L^{-1}$) of the internal standard in the analyzed sample andk_C is the concentration factor (dimensionless) from the step of ABV adjustment.

A.3 Validation of analysis

In order to validate the accuracy and repeatability of the analysis, various global samples of the three process streams were separately analyzed: three in the case of wine and vinasse, and two in the case of distillate, whose matrix composition is relatively clean. Every analysis series was accompanied by three supplementary samples of known composition: (i) one calibration sample to determine the response factor of each volatile aroma compound and (ii) two validation samples for quality control. These samples, prepared at the reference ABV, follow the same analysis path of a real sample, including steam distillation and pretreatment steps, when required.

In Table A3, the real compositions of validation samples are summarized together with the relative errors of the measured values. The real values were determined by weighing. Concerning the analysis by direct injection, the average errors are small, of the order of 1%, for the both ABV ranges. The maximum errors are 6% at low ABV, associated with ethanal, and 9% at high ABV, associated with methanol. For the method with liquid extraction, average errors become higher: 3% at low ABV and 11% at high ABV. The maximum error at low ABV is the associated with ethyl furan-2-carboxylatefuroate, 14%, and at high ABV, with 2-[(2S, 5S)-5-ethenyl-5-methyloxolan-

Table A2 – Quantification limits and response factor of aroma compounds.

Method	Volatile aroma compound	Quantification limit/mg L^{-1}		Response factor	
		Low ABV	High ABV	Low ABV	High ABV
Direct injection-GC/FID	1,1-Diethoxyethane	10.0	10.0	0.5	0.5
	Methanol	10.0	10.0	2.1	1.8
	Prop-2-en-1-ol	5.0	5.0	1.0	1.0
	Propan-1-ol	5.0	5.0	1.2	1.2
	Butan-1-ol	5.0	5.0	1.0	1.0
	Butan-2-ol	5.0	5.0	1.2	1.2
	2-Methylpropan-1-ol	5.0	5.0	1.0	1.0
	2-Methylbutan-1-ol	5.0	5.0	1.0	1.0
	3-Methylbutan-1-ol	5.0	5.0	1.0	1.0
	Ethanal	10.0	10.0	2.6	2.6
	Ethyl ethanoate	10.0	10.0	1.8	1.8
	Ethyl 2-hydroxypropanoate	0.1	5.0	2.0	2.0
	Furan-2-carbaldehyde	5.0	5.0	1.6	1.6
	1,1,3-Triethoxypropane	0.1	0.1	2.3	2.5
	(Z)-Hex-3-en-1-ol	0.1	0.1	3.4	21.9
	Hexan-1-ol	0.1	0.1	2.2	12.6
	Heptan-2-ol	0.1	0.1	15.9	5.7
	2-Phenylethan-1-ol	0.1	0.1	9.7	70.0
	Octan-1-ol	0.1	0.1	2.2	5.2
	Decan-1-ol	0.1	0.1	2.1	2.0
	Dodecan-1-ol	0.1	0.1	2.3	1.3
	Tetradecan-1-ol	0.1	0.1	2.0	1.0
Liquid–liquid extraction- GC/FID	Ethyl butanoate	0.1	0.1	9.0	7.5
	3-Methylbutyl ethanoate	0.1	0.1	3.5	2.1
	(Z)-3-hexenyl ethanoate	0.1	0.1	2.0	1.2
	Ethyl hexanoate	0.1	0.1	2.1	1.1
	Hexyl ethanoate	0.1	0.1	2.2	1.0
	2-Phenylethyl ethanoate	0.1	0.1	3.0	2.3
	Ethyl octanoate	0.1	0.1	2.6	0.8
	Diethyl butane-1,4-dioate	0.1	0.2	9.5	16.2
	Ethyl decanoate	0.1	0.1	4.5	1.2
	3-Methylbutyl octanoate	0.1	0.1	3.5	1.2
	Ethyl dodecanoate	0.1	0.1	2.3	1.1
	2-Phenylethyl octanoate	0.1	0.1	1.9	1.0
	Ethyl tetradecanoate	0.1	0.1	2.0	1.0
	3-methylbutyl dodecanoate	0.1	0.1	2.0	1.0
	Ethyl hexadecanoate	0.1	0.2	1.9	1.0
	Ethyl (9Z,12Z)-9,12-octadecadienoate	0.1	0.1	2.1	1.0
	Ethyl (9Z)-octadec-9-enoate	0.1	0.2	2.0	1.0
	Ethyl octadecanoate	0.1	0.2	3.0	1.6
	Ethyl furan-2-carboxylate	0.1	0.1	8.0	16
	3,7-Dimethylocta-1,6-dien-3-ol	0.1	0.1	1.9	2.5
	2-(4-Methyl-1-cyclohex-3-enyl)propan-2-ol	0.1	0.1	2.1	4.0
Liquid–liquid extraction	2-[(2R,5S)-5-ethenyl-5-methyloxolan-2-yl]propan-2-ol	0.1	0.1	2.4	5.1
	2-[(2S,5S)-5-ethenyl-5-methyloxolan-2-yl]propan-2-ol	0.1	0.1	2.7	6.3
	(Z)-3,7,11-Trimethyl-1,6,10-dodecatrien-3-ol	0.1	0.1	2.1	1.2
	(E)-3,7,11-Trimethyl-1,6,10-dodecatrien-3-ol	0.1	0.1	2.1	1.2
Derivatisation-GC/FID	Methanoic acid	1.0	1.0	3.7	0.8
	Ethanoic acid	1.0	0.1	1.3	0.9
	Propanoic acid	1.0	1.0	4.7	1.0
	Butanoic acid	1.0	1.0	1.9	1.0
	2-Methylpropanoic acid	1.0	1.0	2.4	1.0
	2-Hydroxypropanoic acid	1.0	1.0	4.9	1.3
	2-Methylbutanoic acid	1.0	1.0	3.0	1.1
	3-Methylbutanoic acid	1.0	1.0	3.5	1.0
	Hexanoic acid	1.0	1.0	3.9	1.1
	Octanoic acid	1.0	1.0	5.1	1.2
	Decanoic acid	1.0	1.0	6.4	1.1
	Dodecanoic acid	1.0	1.0	–	1.2
	Tetradecanoic acid	1.0	1.0	–	1.3
	(9Z)-Hexadec-9-enoic acid	1.0	1.0	–	2.0
	Hexadecanoic acid	1.0	1.0	–	1.8
	(9Z,12Z,15Z)-9,12,15-Octadecatrienoic acid	1.0	1.0	–	2.0
	(9Z,12Z)-9,12-Octadecadienoic acid	1.0	1.0	–	1.7
	(9Z)-Octadec-9-enoic acid	1.0	1.0	–	1.6
	Octadecanoic acid	1.0	1.0	–	3.0

Table A3 – Validation of aroma compounds analysis using samples of known composition.

Method	Volatile aroma compound	Low ABV		High ABV	
		Real concentration/mg L^{-1}	Relative deviation/%	Real concentration/mg L^{-1}	Relative deviation/%
Direct injection-GC/FID	1,1-Diethoxyethane	8.1	1%	32.5	1%
	Methanol	50.0	1%	200.0	9%
	Prop-2-en-1-ol	16.1	1%	64.5	0%
	Propan-1-ol	25.7	0%	102.9	0%
	Butan-1-ol	10.1	1%	40.3	1%
	Butan-2-ol	10.1	1%	40.4	0%
	2-Methylpropan-1-ol	37.6	1%	150.4	0%
	2-Methylbutan-1-ol	20.0	0%	79.8	0%
	3-Methylbutan-1-ol	50.0	1%	200.1	0%
	Ethanal	7.8	6%	31.3	6%
	Ethyl ethanoate	60.5	0%	241.8	0%
	Ethyl 2-hydroxypropanoate	20.8	2%	83.3	1%
	Furan-2-carbaldehyde	8.0	1%	32.2	1%
	1,1,3-Triethoxypropane	5.1	3%	5.1	8%
	(Z)-Hex-3-en-1-ol	5.1	4%	5.1	28%
	Hexan-1-ol	5.3	2%	5.3	16%
	Heptan-2-ol	5.2	4%	5.2	3%
	2-Phenylethan-1-ol	2.8	9%	2.8	23%
	Octan-1-ol	5.3	2%	5.3	6%
	Decan-1-ol	5.1	2%	5.1	14%
	Dodecan-1-ol	2.6	3%	2.6	10%
	Tetradecan-1-ol	2.3	2%	2.3	12%
Liquid–liquid extraction- GC/FID	Ethyl butanoate	5.4	5%	5.4	3%
	3-Methylbutyl ethanoate	5.0	1%	5.0	2%
	(Z)-3-hexenyl ethanoate	5.2	1%	5.2	7%
	Ethyl hexanoate	5.1	1%	5.1	4%
	Hexyl ethanoate	5.1	3%	5.1	4%
	2-Phenylethyl ethanoate	5.1	2%	5.1	3%
	Ethyl octanoate	5.2	1%	5.2	4%
	Diethyl butane-1,4-dioate	5.4	7%	5.4	13%
	Ethyl decanoate	5.2	1%	5.2	9%
	3-Methylbutyl octanoate	4.9	2%	4.9	12%
	Ethyl dodecanoate	2.6	2%	2.6	2%
	2-Phenylethyl octanoate	2.6	2%	2.6	3%
	Ethyl tetradecanoate	2.7	2%	2.7	7%
	3-methylbutyl dodecanoate	2.5	3%	2.5	9%
	Ethyl hexadecanoate	2.9	0%	2.9	14%
	Ethyl (9Z,12Z)-9,12-octadecadienoate	2.4	2%	2.4	17%
	Ethyl (9Z)-octadec-9-enoate	2.3	1%	2.3	18%
	Ethyl octadecanoate	3.8	2%	3.8	15%
	Ethyl furan-2-carboxylate	5.0	14%	5.0	16%
	3,7-Dimethylocta-1,6-dien-3-ol	5.4	1%	5.4	9%
	2-(4-Methyl-1-cyclohex-3-enyl)propan-2-ol	5.0	2%	5.0	12%
	2-[(2R,5S)-5-ethenyl-5-methyloxolan-2-yl]propan-2-ol	2.8	1%	2.8	31%
	2-[(2S,5S)-5-ethenyl-5-methyloxolan-2-yl]propan-2-ol	2.3	2%	2.3	34%
	(Z)-3,7,11-Trimethyl-1,6,10-dodecatrien-3-ol	0.9	1%	0.9	0%
	(E)-3,7,11-Trimethyl-1,6,10-dodecatrien-3-ol	1.2	1%	1.2	2%
Derivatization-GC/FID	Methanoic acid	101.8	12%	102.9	11%
	Ethanoic acid	99.0	15%	104.4	6%
	Propanoic acid	97.9	33%	97.5	3%
	Butanoic acid	99.9	15%	99.4	4%
	2-Methylpropanoic acid	99.7	6%	103.2	1%
	2-Hydroxypropanoic acid	98.8	48%	83.5	3%
	2-Methylbutanoic acid	100.5	8%	102.1	4%
	3-Methylbutanoic acid	100.5	11%	104.5	5%
	Hexanoic acid	101.7	23%	103.8	2%
	Octanoic acid	98.5	29%	105.8	1%
	Decanoic acid	98.4	17%	95.0	4%
	Dodecanoic acid	–	–	46.6	9%
	Tetradecanoic acid	–	–	48.9	1%
	(9Z)-Hexadec-9-enoic acid	–	–	56.3	20%
	Hexadecanoic acid	–	–	47.4	7%
	(9Z,12Z,15Z)-9,12,15-Octadecatrienoic acid	–	–	50.3	4%
	(9Z,12Z)-9,12-Octadecadienoic acid	–	–	47.9	6%
	(9Z)-Octadec-9-enoic acid	–	–	58.8	9%
	Octadecanoic acid	–	–	47.5	8%

2-yl] propan-2-ol (trans-linalool oxide), equivalent to 34%. For the derivatization method, the average deviations are 20% at low ABV and 6% at high ABV. The maximum errors are 48% at low ABV, related to 2-hydroxypropanoic acid (lactic acid), and 20% at high ABV, corresponding to (9Z)-hexadec-9-enoic acid (palmitoleic acid).

References

Allen, G., Caldin, E.F., 1953. The association of carboxylic acids. Q. Rev. Chem. Soc. 7, 255–278.

Apostolopoulou, A.A., Flouros, A.I., Demertzis, P.G., Akrida-Demertzi, K., 2005. Differences in concentration of principal volatile constituents in traditional Greek distillates. Food Control 16, 157–164.

Arce, A., Martinez-Ageitos, J., Soto, A., 1996. VLE for water + ethanol + 1-octanol mixtures. Experimental measurements and correlations. Fluid Phase Equilib. 122, 117–129.

Athès, V., Paricaud, P., Ellaite, M., Souchon, I., Fürst, W., 2008. Vapour–liquid equilibria of aroma compounds in hydroalcoholic solutions: measurements with a recirculation method and modelling with the NRTL and COSMO-SAC approaches. Fluid Phase Equilib. 265, 139–154.

Awad, P., Athès, V., Decloux, M., Ferrari, G., Snakkers, G., Raguenaud, P., Giampaoli, P., 2017. Evolution of volatile compounds during the distillation of cognac spirit. J. Agri. Food Chem. 65 (35), 7736–7748.

Bastidas, P., Parra, J., Gil, I., Rodriguez, G., 2012. Alcohol distillation plant simulation: thermal and hydraulic studies. Procedia Eng. 42, 80–89.

Batista, R.M., Meirelles, A.J.A., 2009. A strategy for controlling acetaldehyde content in an industrial plant of bioethanol. IFAC Proc. Volumes 42 (11), 928–933.

Batista, F.R.M., Meirelles, A.J.A., 2011. Computer simulation applied to studying continuous spirit distillation and product quality control. Food Control 22, 1592–1603.

Batista, F.R.M., Follegatti-Romero, L.A., Bessa, L.C.B.A., Meirelles, A.J.A., 2012. Computational simulation applied to the investigation of industrial plants for bioethanol distillation. Comput. Chem. Eng. 46, 1–16.

Batista, F.R.M., Follegatti-Romero, L.A., Meirelles, A.J.A., 2013. A new distillation plant for natural alcohol production. Sep. Purif. Technol. 118, 784–793.

Bertrand, A., Ségur, M.C., Jadeau, P., 1998. Comparaison analytique des eaux-de-vie déArmagnac obtenues par distillation continue et double chauffe. Connaissance Vigne Vin 22 (1), 89–92.

Bertrand, A., 2003. Armagnac and Wine-Spirits. In: Lea, A.G.H., Piggott, J.R. (Eds.), Fermented Beverage Production, Second ed. Kluwer Academic/Plenum Publishers, New York, pp. 213–238.

Bon, J., Clemente, G., Vaquiro, H., Mulet, A., 2009. Simulation and optimization of milk pasteurization processes using general process simulator (ProSimPlus). Comput. Chem. Eng. 34, 414–420.

Cacho, J., Moncayo, L., Palma, J.C., Ferreira, V., Culleré, L., 2013. The influence of different production processes on the aromatic composition of Peruvian Piscos. J. Nutr. Food Sci. 3 (6), 1–10.

Cantagrel, R., Lurton, L., Vidal, J.-P., Galy, B., 1990. La distillation charentaise pour l'obtention des eaux-de-vie de Cognac. In: Bertrand, A. (Ed.), Les eaux-de-vie traditionnelles d'origine viticole. Technique et Documentation, Bordeaux.

Carrau, F., Medina, K., Farina, L., Boido, E., Henschke, P., Dellacassa, E., 2008. Production of fermentation aroma compounds by *Saccharomyces cerevisiae* wine yeasts: effects of yeast assimilable nitrogen on two model strains. FEMS Yeast Res. 8, 1196–1207.

Carvallo, J., Labbe, M., Pérez-Correa, J.R., Zaror, C., Wisniak, J., 2011. Modeling methanol recovery in wine distillation stills with packing columns. Food Control 22, 1322–1332.

Çengel, Y., 2007. Heat and Mass Transfer, 3rd ed. McGraw Hill, Mexico.

Claus, M.J., Berglund, K.A., 2009. Defining still parameters using ChemCAD batch distillation model for modeling fruit spirits distillations. J. Food Process Eng. 32, 881–892.

Day, J., 2012. Laminar natural convection from isothermal vertical cylinders, MSc. Thesis. University of North Texas, Denton, Available from: https://digital.library.unt.edu/ark:/67531/metadc177190/m2/1/high_res_d/thesis.pdf. Accessed 15-12-2015.

Decloux, M., Coustel, J., 2005. Simulation of a neutral spirit production plant using beer distillation. Int. Sugar J. 107 (1283), 628–643.

Decloux, M., Joulia, X., 2009. Distillation of AOC French spirits: Cognac, Armagnac, Calvados and Martinique agricultural rum. In: Ingledew, W.M., Kelsall, D.R., Austin, G.D., Kluhspies, C. (Eds.), The Alcohol Textbook. , Fifth ed. Nottingham University Press, Nottingham, pp. 491–506.

Detcheberry, M., Destrac, P., Massebeuf, S., Baudouin, O., Gerbaud, V., Condoret, J.-S., Meyer, X.-M., 2016. Thermodynamic modeling of the condensable fraction of a gaseous effluent from lignocellulosic biomass torrefaction. Fluid Phase Equilibr. 409, 242–255.

Esteban-Decloux, M., Deterre, S., Kadir, S., Giampaoli, P., Albet, J., Joulia, X., Baudouin, O., 2014. Two industrial examples of coupling experiments and simulations for increasing quality and yield of distilled beverages. Food Bioprod. Process. 92, 343–354.

Faúndez, C.A., Valderrama, J.O., 2004. Phase equilibrium modeling in binary mixtures found in wine and must distillation. J. Food Eng. 65, 577–583.

Faúndez, C.A., Alvarez, V.H., Valderrama, J.O., 2006. Predictive models to describe VLE in ternary mixtures water + ethanol + congener for wine distillation. Thermochim. Acta 450, 110–117.

Faúndez, C.A., Valderrama, J.O., 2009. Activity coefficient models to describe vapor-liquid equilibrium in ternary hydro-alcoholic solutions. Chin. J. Chem. 17, 259–267.

Ferrari, G., Lablanquie, O., Cantagrel, R., Ledauphin, J., Payot, T., Fournier, N., Guichard, E., 2004. Determination of key odorant compounds in freshly distilled Cognac using GC-O, GC-MS, and sensory evaluation. J. Agric. Food Chem. 52, 5670–5676.

Franitza, L., Granvogl, M., Schieberle, P., 2016. Influence of the production process on the key volatile aroma compounds of rum: from molasses to the spirit. J. Agric. Food Chem. 64, 9041–9053.

Gaiser, M., Bell, G.M., Lim, A.W., Roberts, N.A., Faraday, D.B.F., Schulz, R.A., Grob, R., 2002. Computer simulation of a continuous whisky still. J. of Food Eng. 51, 27–31.

Gil, I.D., Guevara, J.R., García, J.L., Leguizamón, A., 2011. Análisis y simulación de procesos en Ingeniería Química, First ed. Editorial Universidad Nacional de Colombia, Bogotá.

Gmehling, J., Li, J., Schiller, M., 1993. A modified UNIFAC model. 2. Present parameter matrix and results for different thermodynamic properties. Ind. Eng. Chem. Res. 32, 178–193.

Guichard, H., Lemesle, S., Ledauphin, J., Barillier, D., Picoche, B., 2003. Chemical and sensorial aroma characterization of freshly distilled calvados 1. Evaluation of quality and defects on the basis of key odorants by olfactometry and sensory analysis. J. Agric. Food Chem. 51, 424–432.

Guymon, J., 1974. Chemical aspects of distilling wine into brandy. In: Chemistry of Winemaking, Webb,A., Advances in Chemistry. American Chemical Society, Washington, pp. 232–253.

Heyen, G. and Arpentinier, P., Validation et réconciliation de données mesurées sur une installation industrielle, Tutoriel 11, 16ème Congrès de la Société Française de Génie des Procédés, 2017; Nancy.

JORF, Cahier des charges de l'appellation d'origine contrôlée Armagnac homologué par le décret n°2014–1642 du 26 décembre 2014, Journal Officiel de la République Française, 2015; Paris. Available from: https://info.agriculture.gouv.fr/gedei/site/bo-agri/document_administratif-3cd649de-17de-4c86-bf84-92b2669483af. Accessed 05-01-2016.

Joulia, X., Simulateurs de procédés, Techniques de l'ingénieur J1022, 2008, 1–25.
Kadir, S., 2009. Optimisation du procédé de production d'Alcool surfin, PhD Thesis. AgroParisTech, Paris, Available from: https://infodoc.agroparistech.fr/index.php?lvl=notice_display&id=187425. Accessed 05-11-2014.
Kamihama, N., Matsuda, H., Kurihara, K., Tochigi, K., Oba, S., 2012. Isobaric vapor-liquid equilibria for ethanol + water + ethylene glycol and its constituent three binary systems. J. Chem. Engi. Data 57, 339–344.
Kister, H.Z., 1992. Distillation design, First ed. McGraw-Hill Education, New York.
Lai, H.-S., Lin, Y.-F., Tu, C.-H., 2014. Isobaric (vapor + liquid) equilibria for the ternary system of (ethanol + water + 1,3-propanediol) and three constituent binary systems at P = 101.3 kPa. J. Chem. Thermodyn. 68, 13–19.
Ledauphin, J., Basset, B., Cohen, S., Payot, T., Barillier, D., 2006. Identification of trace volatile compounds in freshly distilled Calvados and Cognac: Carbonyl and sulphur compounds. J. Food Compos. Anal. 19, 28–40.
Ledauphin, J., Le Milbeau, C., Barillier, D., Hennequin, D., 2010. Differences in the volatile compositions of French Llabeled brandies (Armagnac, Calvados, Cognac, and Mirabelle) using GC–MS and PLS-DA. J. Agric. Food Chem. 58, 7782–7793.
Maarse, H., Van Den Berg, F., 1994. Flavour of distilled beverages. In: Paterson, J.R., First, A. (Eds.), Understanding of natural flavors, Piggott. Springer Science + Business Media Dordetch, London, pp. 243–267.
MacNamara, K., Hoffmann, A., 1998. Gas chromatography technology in analysis of distilled spirits. In: Wetzel, D., Charalambous, G. (Eds.), Instrumental methods in food and beverage. Elsevier, Amsterdam, pp. 303–346.
MacNamara, K., Lee, M., Robbat, A., 2010. Rapid gas chromatographic analysis of less abundant compounds in distilled spirits by direct injection with ethanol–water venting and mass spectrometric data deconvolution. J. Chromatogr. A 1217, 136–142.
Marty and Cluzeau, Diagnostic énergétique dans l'Armagnac, synthèse audit énergétique, 2010, AD'3E; Castres.
Morakul, S., Mouret, J.-R., Nicolle, P., Trelea, I., Sablayrolles, J.-M., Athès, V., 2011. Modelling of the gas–liquid partitioning of aroma compounds during wine alcoholic fermentation and prediction of aroma losses. Process Biochem. 46, 1125–1131.
Nykänen, L., 1986. Formation and occurrence of flavor compounds in wine and distilled alcoholic beverages. Am. J. Enol. Vitic. 37 (1), 84–96.
Nykänien, L., Suomalainen, H., 1983. Aroma of Beer, Wine and Distilled Alcoholic Beverages. D. Reidel Publishing Company, Dordretch.
OIML, International alcoholometric tables, R 22, International Organization of Legal Metrology, 1975; Paris. Available from: http://www.itecref.com/pdf/OIML_Alcoholometric_Tables.pdf. Accessed 12-06-2016.
OIV, Recueil des méthodes internationales des boissons spiritueuses d'origine vitivinicole, International Organisation of Vine and Wine, 2014; Paris. Available from: http://www.oiv.int/public/medias/2626/recueil-bs-2014-pdf-complet-fr.pdf. Accessed 12-06-2016.
OIV, Compendium of international methods of wine and must analysis, International Organisation of Vine and Wine, 2016; Paris. Available from: http://www.oiv.int/public/medias/4231/compendium-2016-en-vol1.pdf. Accessed 12-06-2016.
Osorio, D., Pérez-Correa, R., Belancic, A., Agosin, E., 2004. Rigorous dynamic modeling and simulation of wine distillations. Food Control 15, 515–521.
Oudin, P., 1980. Guide pratique d'alcoométrie. Ed Oudin, Poitiers.
Paine, A.J., Dayan, A.D., 2001. Defining a tolerable concentration of methanol in alcoholic drinks. Hum Exp. Toxicol. 20, 563–568.
Piggott, J., 2009. Distillation of brandies. In: Ingledew, W.M., Kelsall, D.R., Austin, G.D., Kluhspies, C. (Eds.), The Alcohol Textbook, fifth ed. Nottingham University Press, Nottingham, pp. 491–506.
Puentes, C., Joulia, X., Athès, V., Esteban-Decloux, M., 2018a. Review and thermodynamic modeling with NRTL model of vapor-liquid equilibria (VLE) of volatile aroma compounds highly diluted in ethanol–water mixtures at 101.3 kPa. Ind. Eng. Chem. Res. 57, 3443–3470.
Puentes, C., Joulia, X., Paricaud, P., Giampaoli, P., Athès, V., Esteban-Decloux, M., 2018. Vapor-liquid equilibrium (VLE) of ethyl lactate highly diluted in ethanol–water solutions at 101.3 kPa: experimental measurements and thermodynamic modeling with semi-empiric models. J. Chem. Eng. Data 63, 365–379.
Renon, H., Prausnitz, J.M., 1968. Local compositions in thermodynamic excess functions for liquid mixtures. AIChE J. 14, 135–144.
Rodriguez, R., Blanco, D., Mangas, J., 2003. Influence of distillation system, oak wood type, and aging time on volatile compounds of cider brandy. J. Agric. Food Chem. 51, 5709–5714.
Sacher, J., García-Llobodanin, L., López, F., Segura, H., Pérez-Correa, J.R., 2013. Dynamic modeling and simulation of an alembic pear wine distillation. Food and Bioprod. Process. 91, 447–456.
Scanavini, H.F.A., Ceriani, R., Cassini, C.E.B., Souza, E.L.R., Maugeri-Falco, F., Meirelles, A.J.A., 2010. Cachaça production in a lab-scale alembic: Modeling and computational simulation. J. Food Process Eng. 33, 226–252.
Scanavini, H.F.A., Ceriani, R., Meirelles, A.J.A., 2012. Cachaça distillation investigated on the basis of model systems. Braz. J. Chem. Eng. 29 (02), 429–440.
Segur, M.C., Bertrand, A., 1992. La distillation continue armagnacais (continous Armagnac distillation). In: Cantagrel, R. (Ed.), Elaboration et connaissances des Spiritieux (Elaboration and knowledge of spirit beverages). Lavoisir Tec et Doc, Paris, pp. 257–266.
Sourisseau, J., 2002. Etude chimique de la distillation du cognac. Bulletin de l'Union des Physiciens 96, 881–892.
Tgarguifa, A., Abderafi, S., Bounahmidi, T., 2017. Energetic optimization of Moroccan distillery using simulation and response surface methodology. Renewable Sustainable Energy Rev. 76, 415–425.
Valderrama, J.O., Faúndez, C.A., 2003. Modeling of vapor–liquid equilibrium in binary and ternary mixtures of interest in alcoholic distillation. Información Tecnológica 14 (1), 83–92.
Valderrama, J.O., Faúndez, C.A., Toselli, L.A., 2012a. Advances on modeling and simulation of alcoholic distillation.Part 1: Thermodynamic modeling. Food and Bioprod. Process. 90, 819–831.
Valderrama, J.O., Toselli, L.A., Faúndez, C.A., 2012b. Advances on modeling and simulation of alcoholic distillation. Part 2: Process simulation. Food and Bioprod. Process. 90, 832–840.
Vawdrey, A.C., Oscarson, J.L., Rowley, R.L., Wilding, W.V., 2004. Vapor-phase association of n-aliphatic carboxylic acids. Fluid Phase Equilibria 222–223, 239–245.
Vrielynck, B., 2002. Les procédés mieux maîtrisés grâce à la réconciliation de données. Mesures 741, 30–34.
Yang, B., Wang, H., 2002. Vapor–liquid equilibrium for mixtures of water, alcohols, and ethers. J. Chem. Eng. Data 47, 1324–1329.